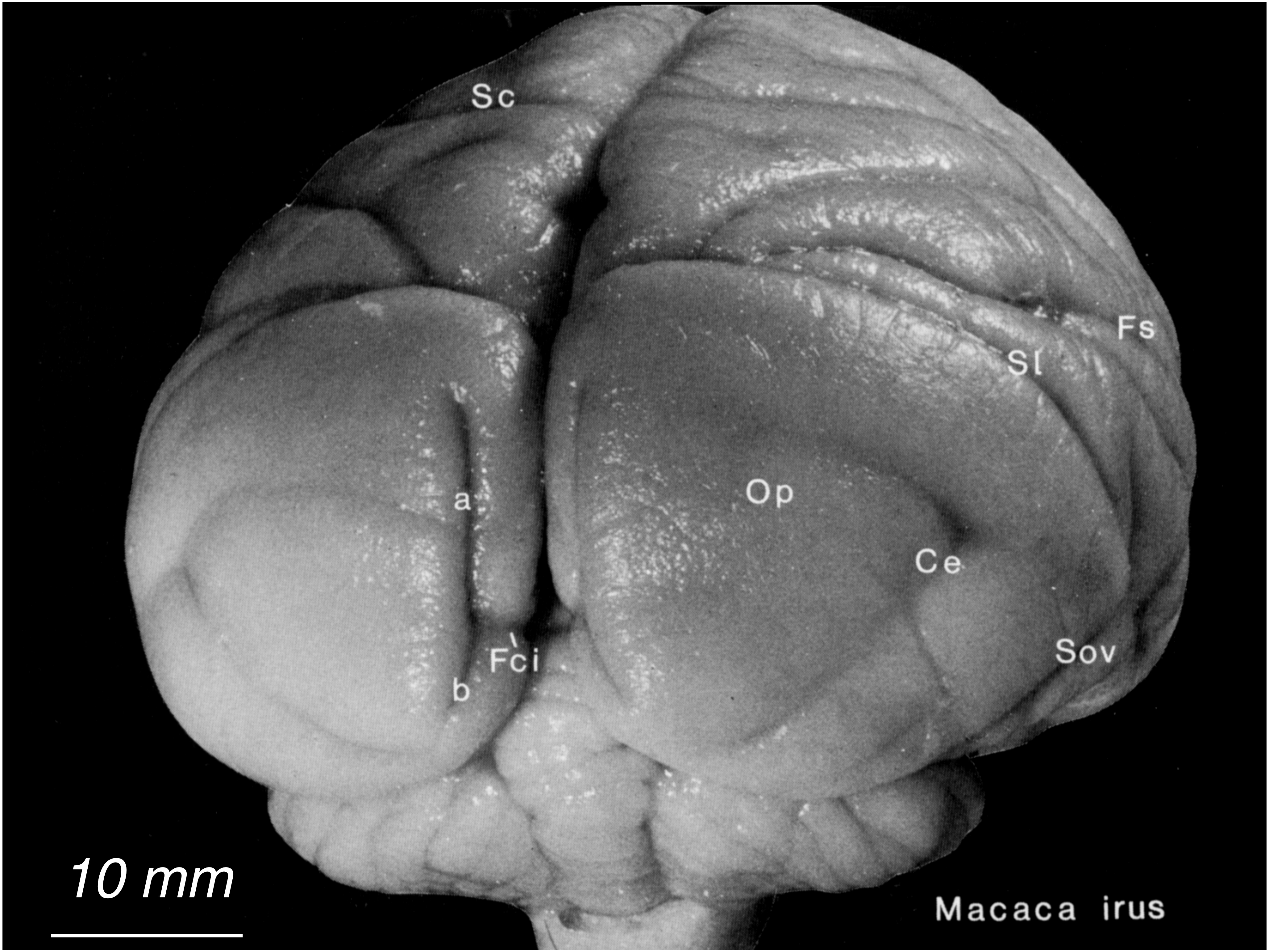
Sc
Fs
Sl
a
Op
Ce
Fci
b
Sov
10 mm
Macaca irus

Cytoarchitecture and function

layer 4: input

layer 5: output

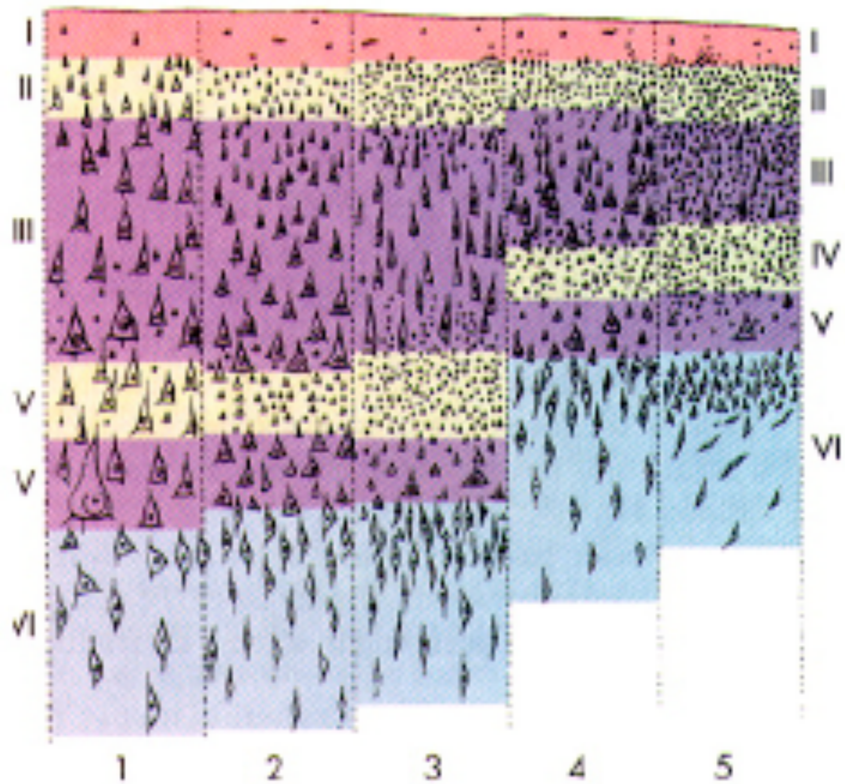

Motor cortex: expanded layer 5, reduced layer 4

Primary visual cortex: expanded layer 4 with three sublayers

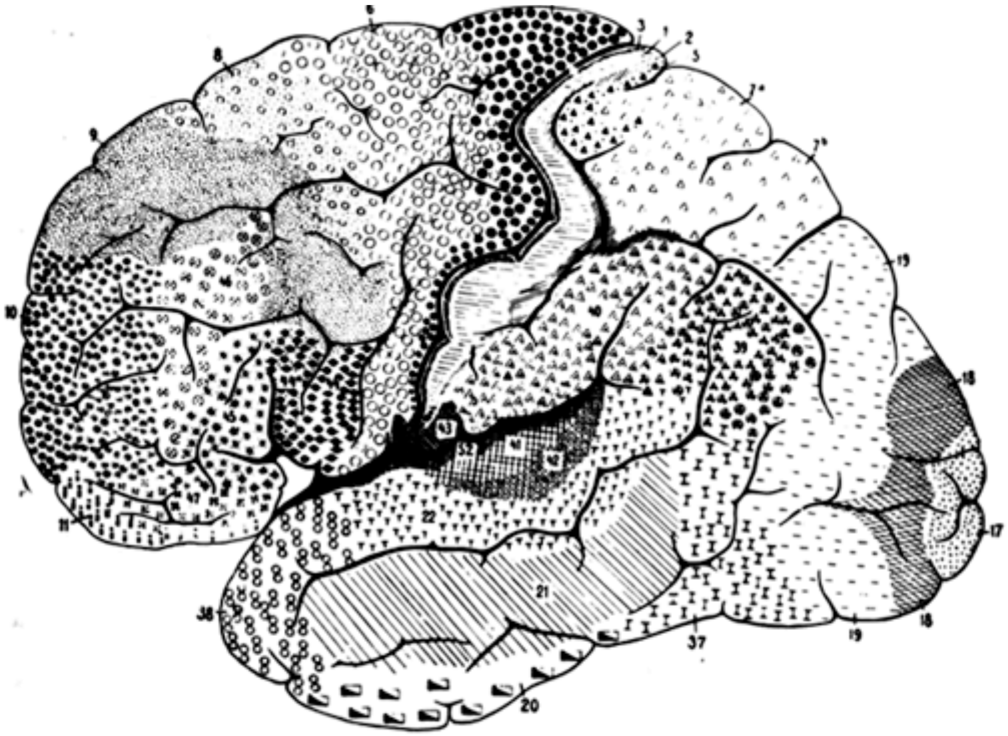

Abb. 6.

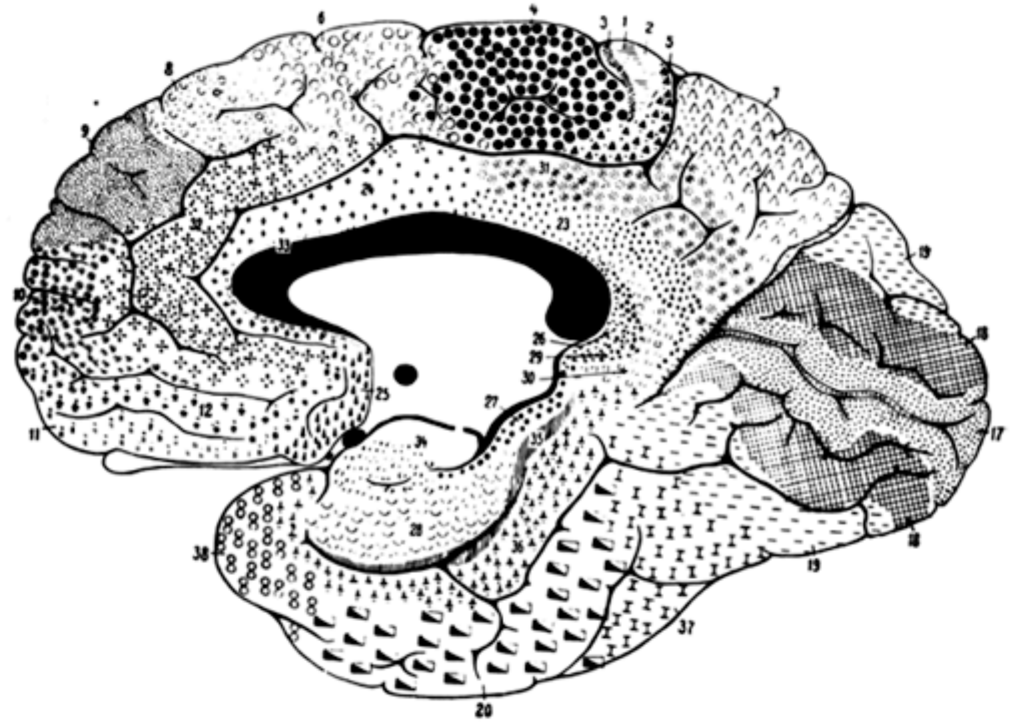

Abb. 7.

Macaque V1

Myelin

Nissl

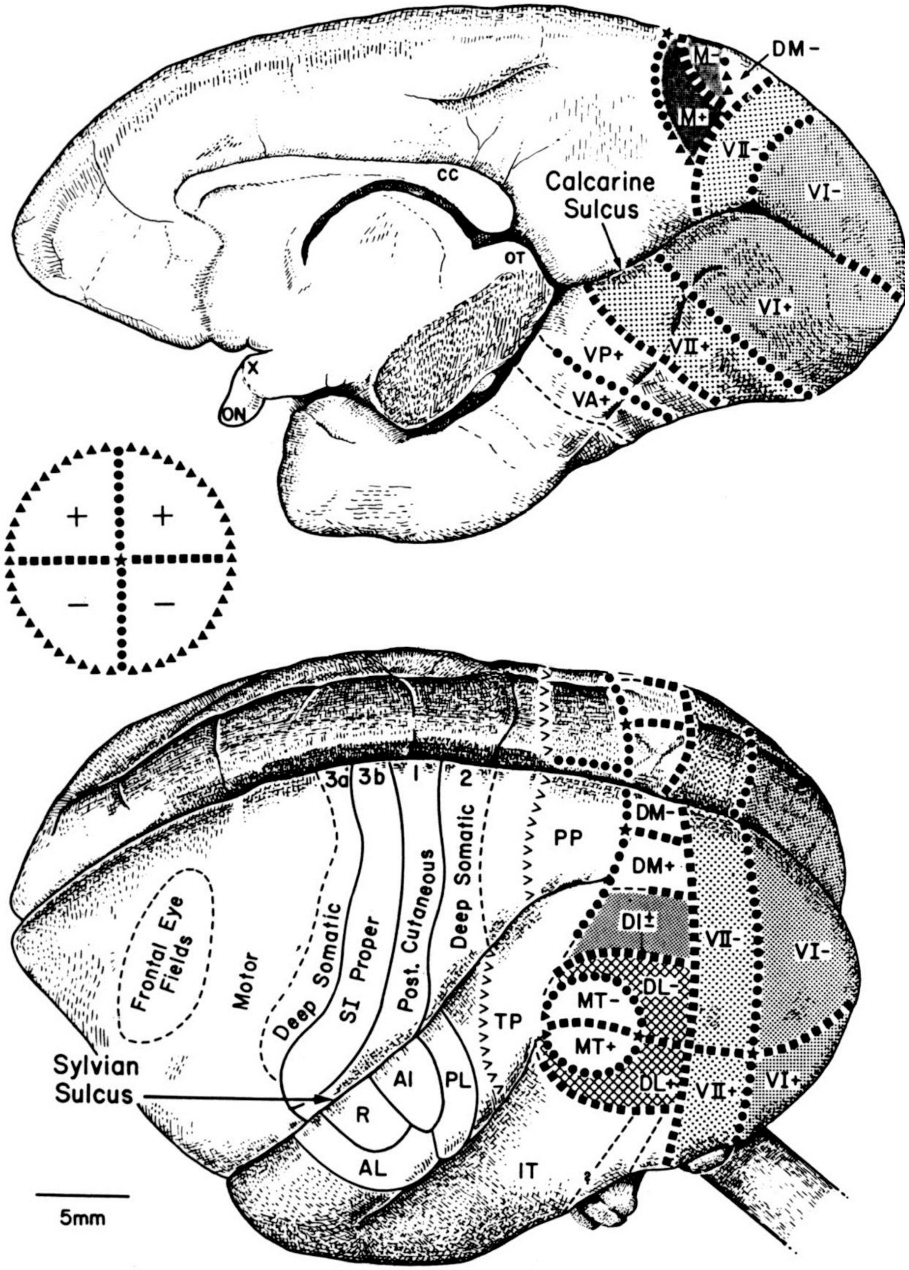

Allman & Kaas, 1981

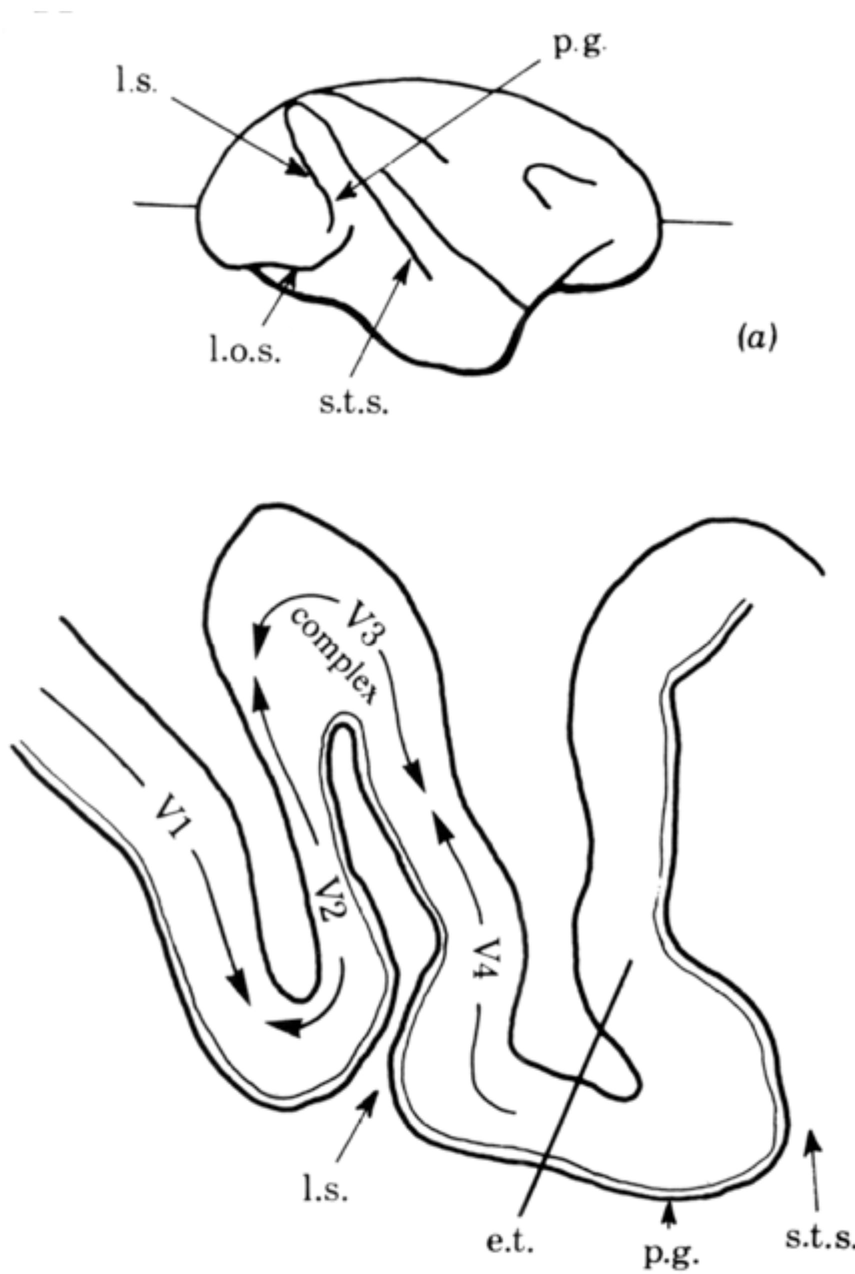

Zeki, 1978

Physically flattening the macaque brain

Sincich, Adams & Horton (2003)

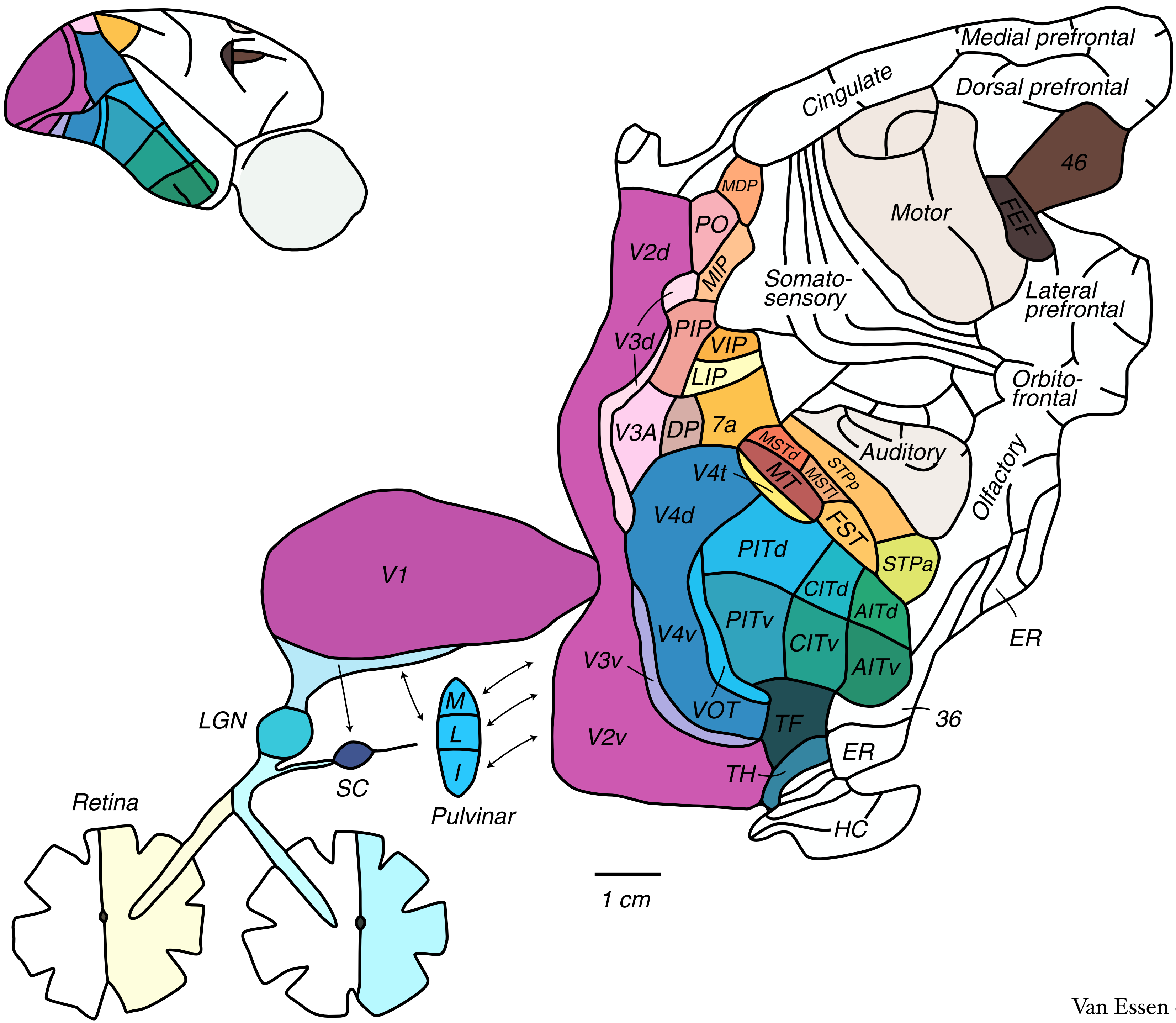

Van Essen et al., 1992

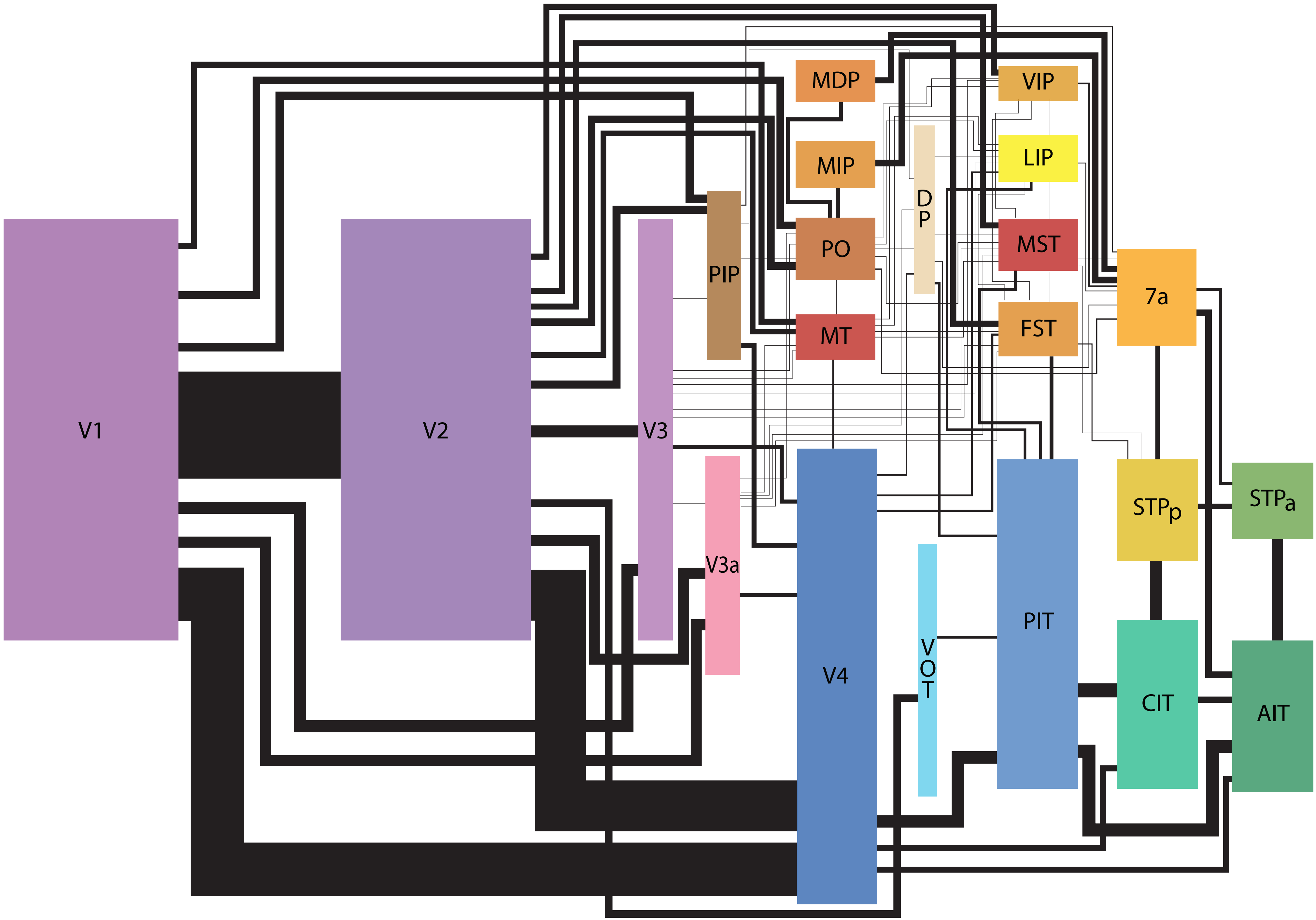

Wallisch & Movshon, 2008

after Felleman & Van Essen, 1991

Computationally flattening the human brain

David Van Essen

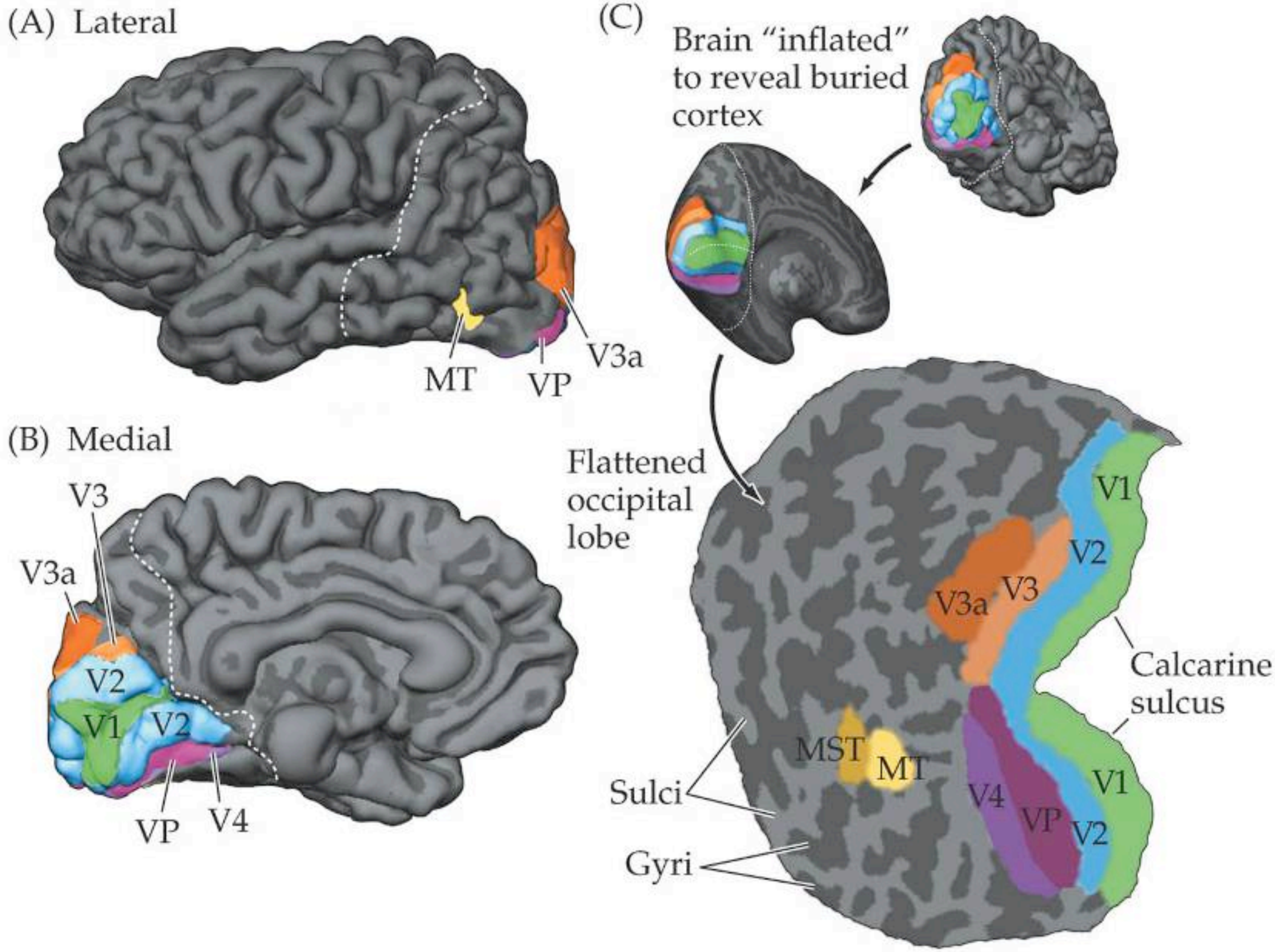

NEUROSCIENCE, Third Edition, Figure 11.16

Inflating and flattening the human cortex (Tootell and Dale)

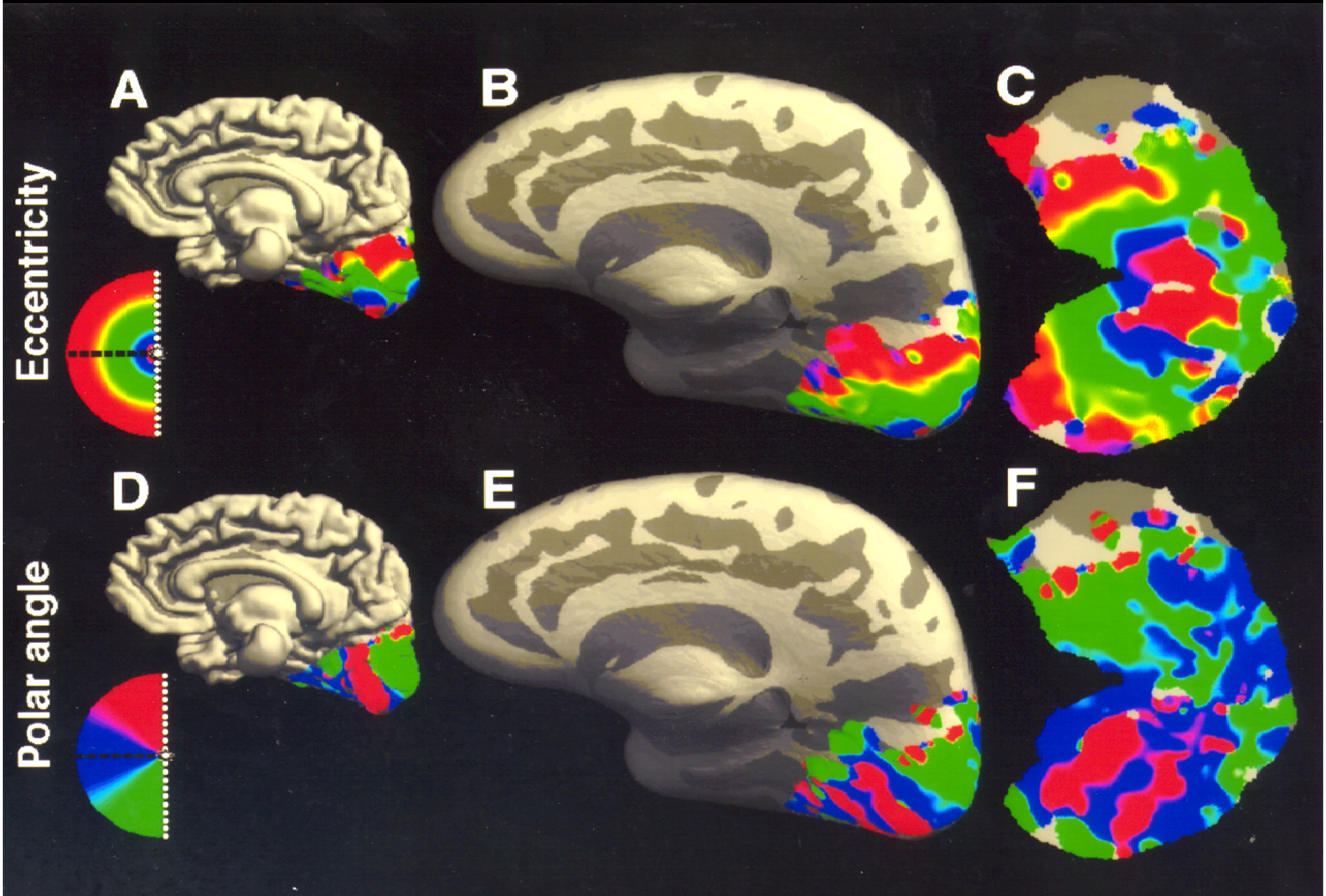

Retinotopy (human V1)

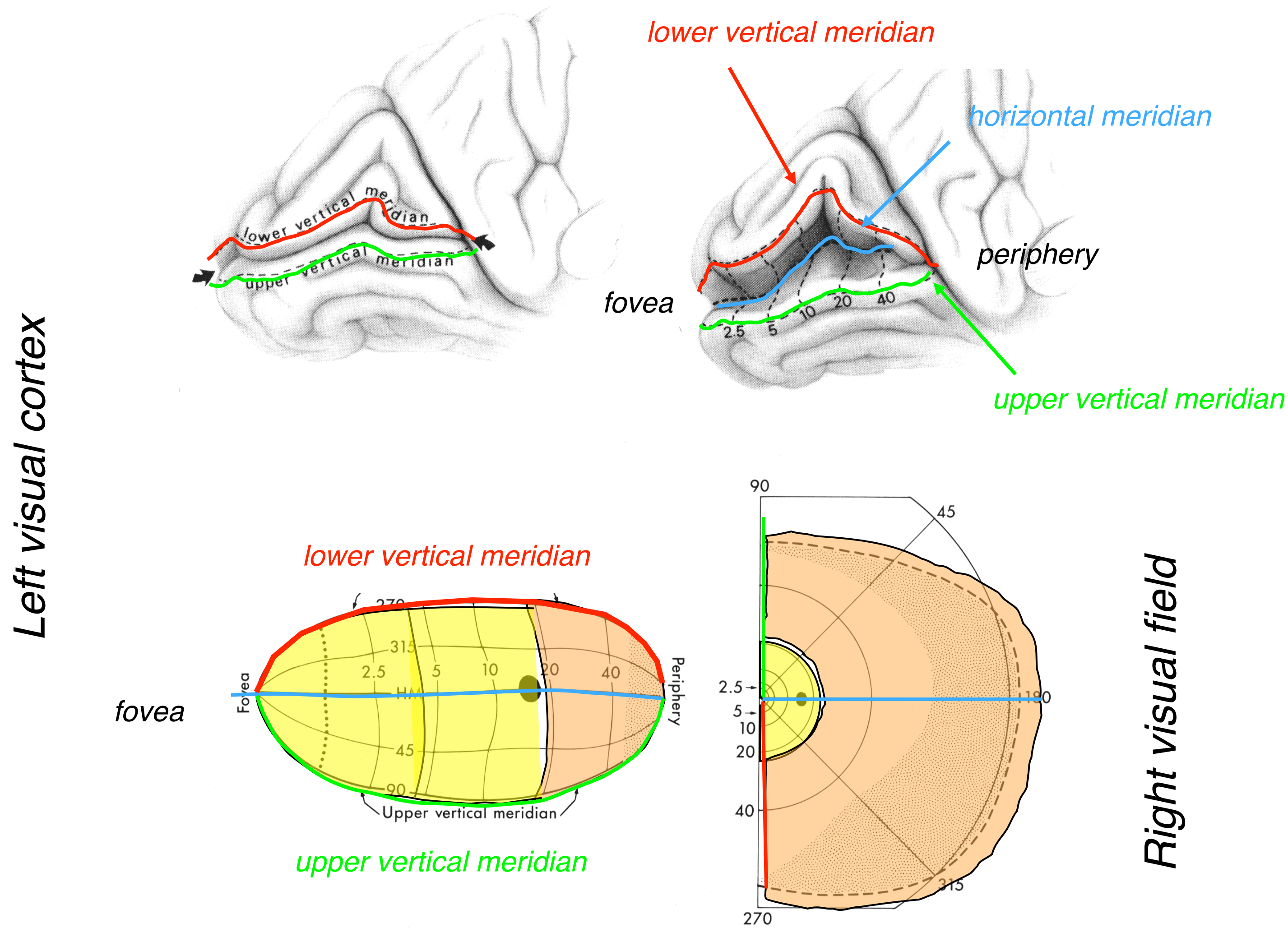

Cortical magnification

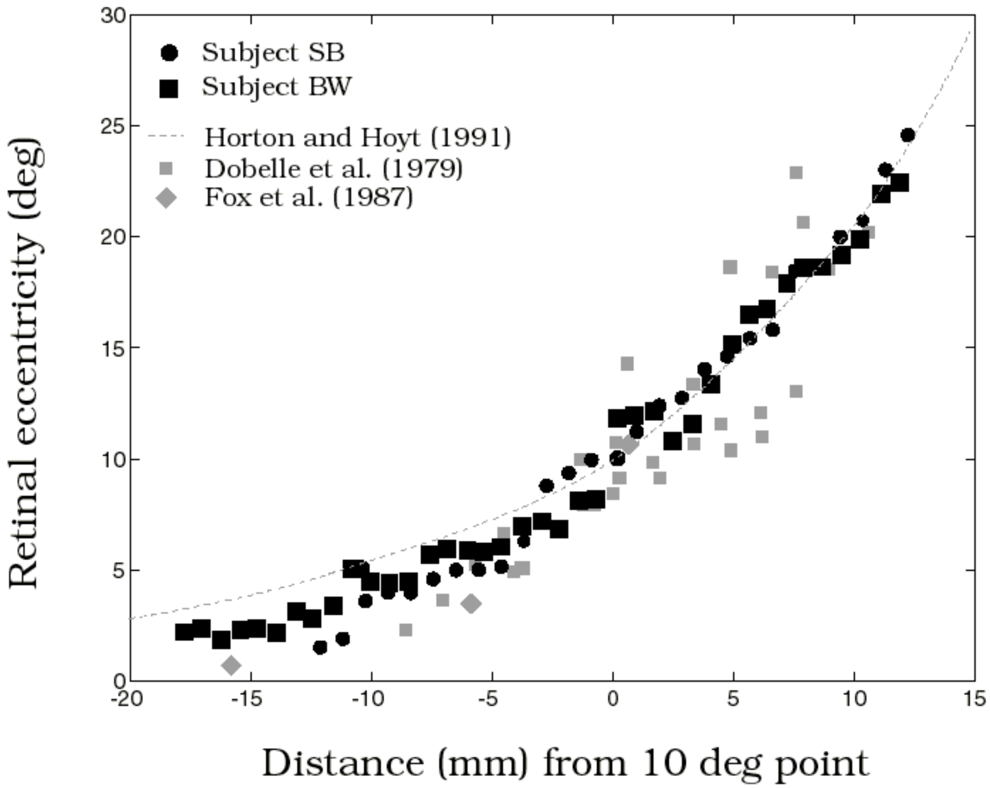

Engel, Glover, & Wandell, Cereb Cortex (1997)

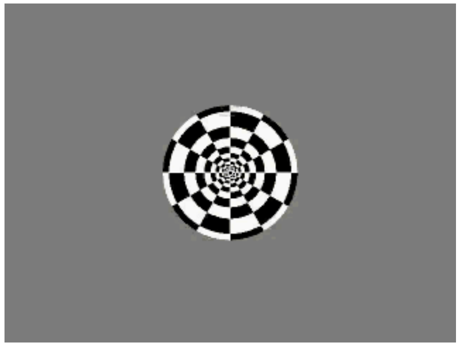

Human visual areas

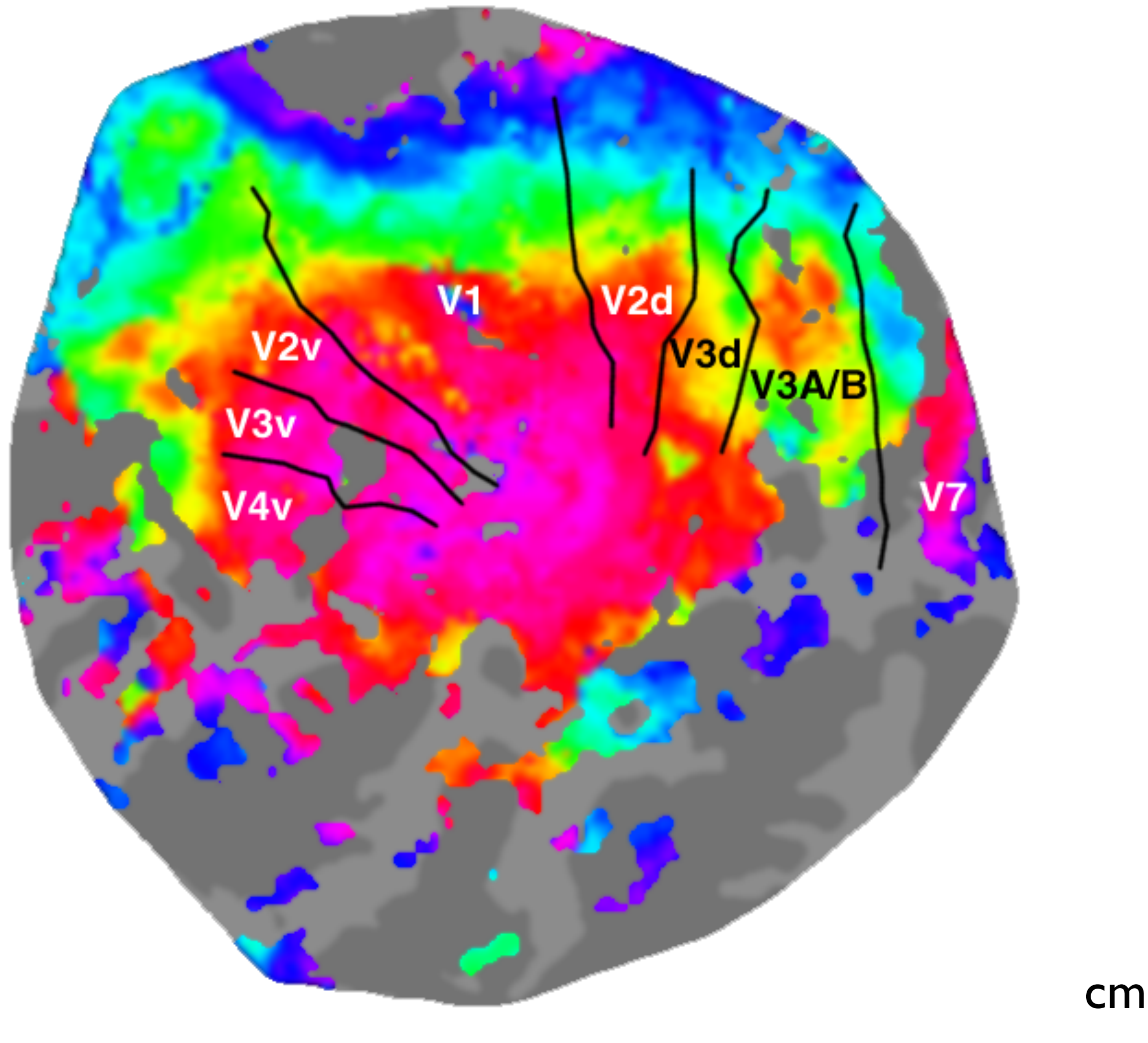

Brian Wandell

Human visual areas

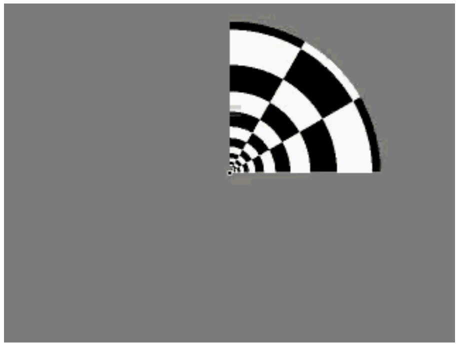

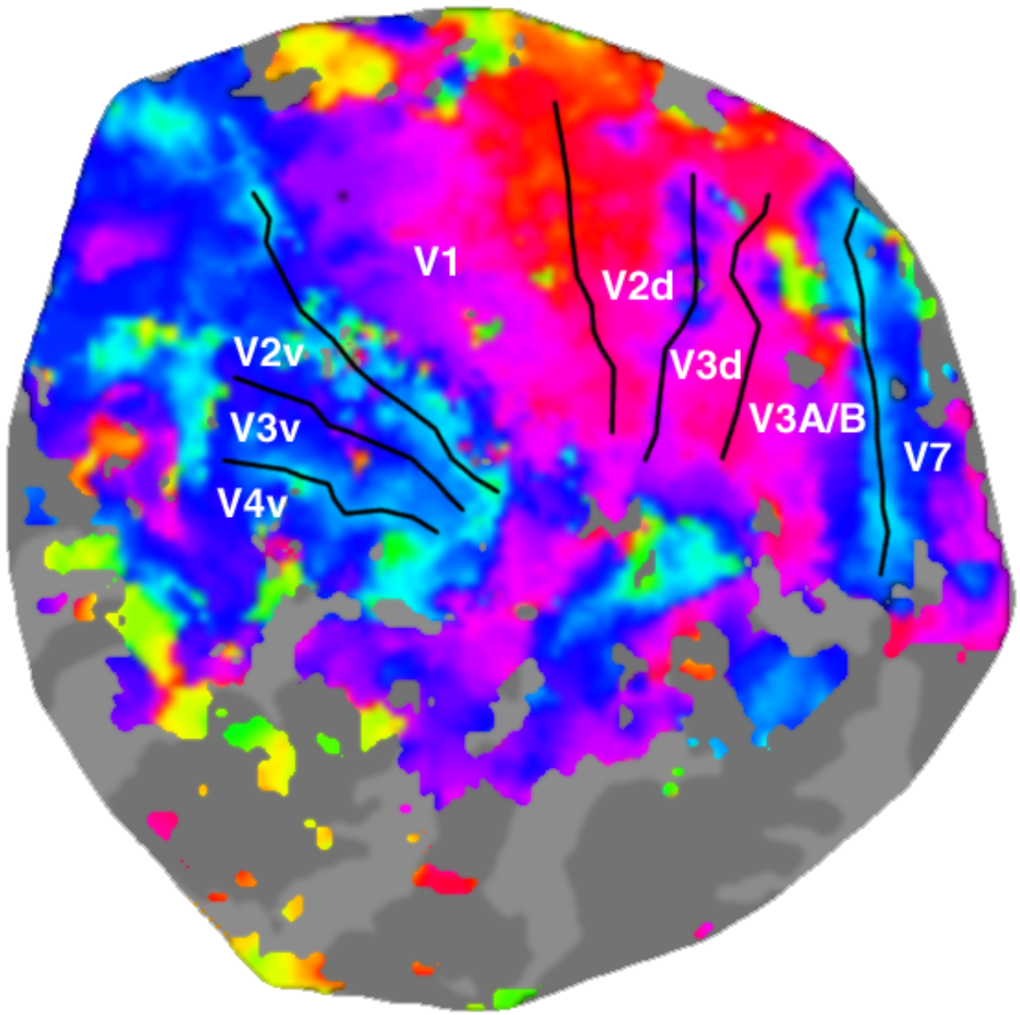

cm

Brian Wandell

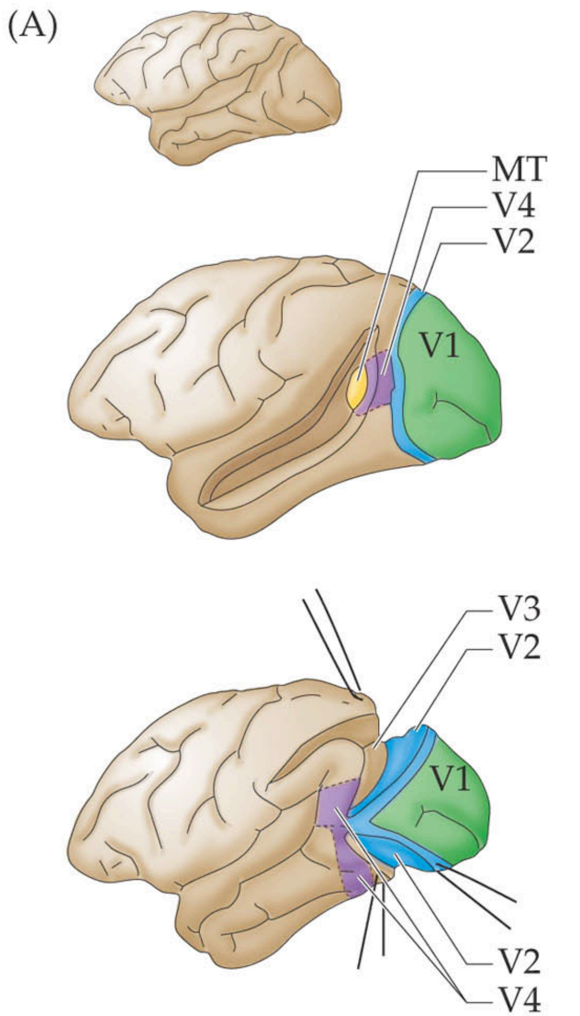

NEUROSCIENCE, Thi

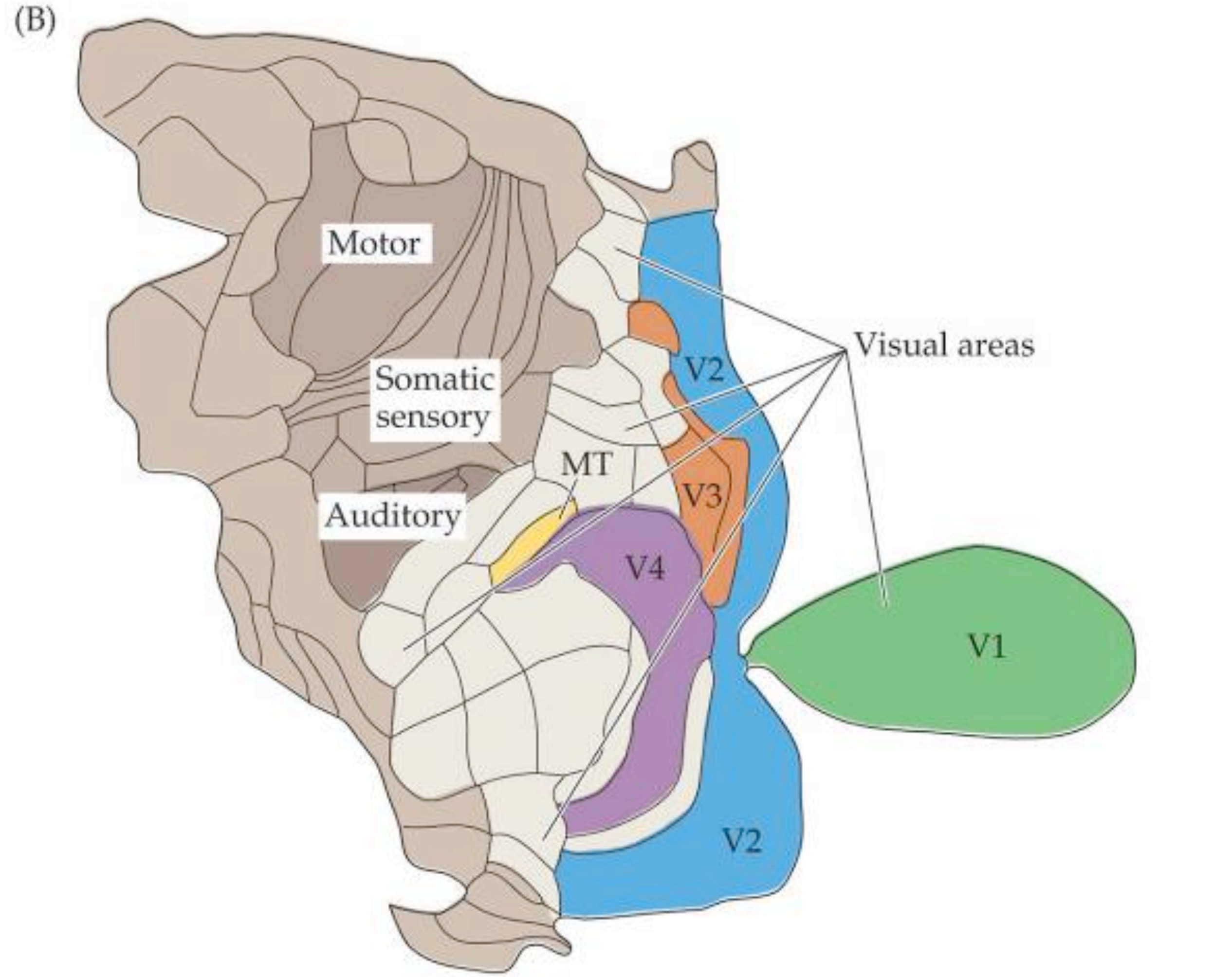

NEUROSCIENCE, Third Edition, Figure 11.15 (Part 2) © 2004 Sinauer Associates, Inc.

A comparison of cortical visual areas in humans and two other primate species. After Tootell and Dale (1996).

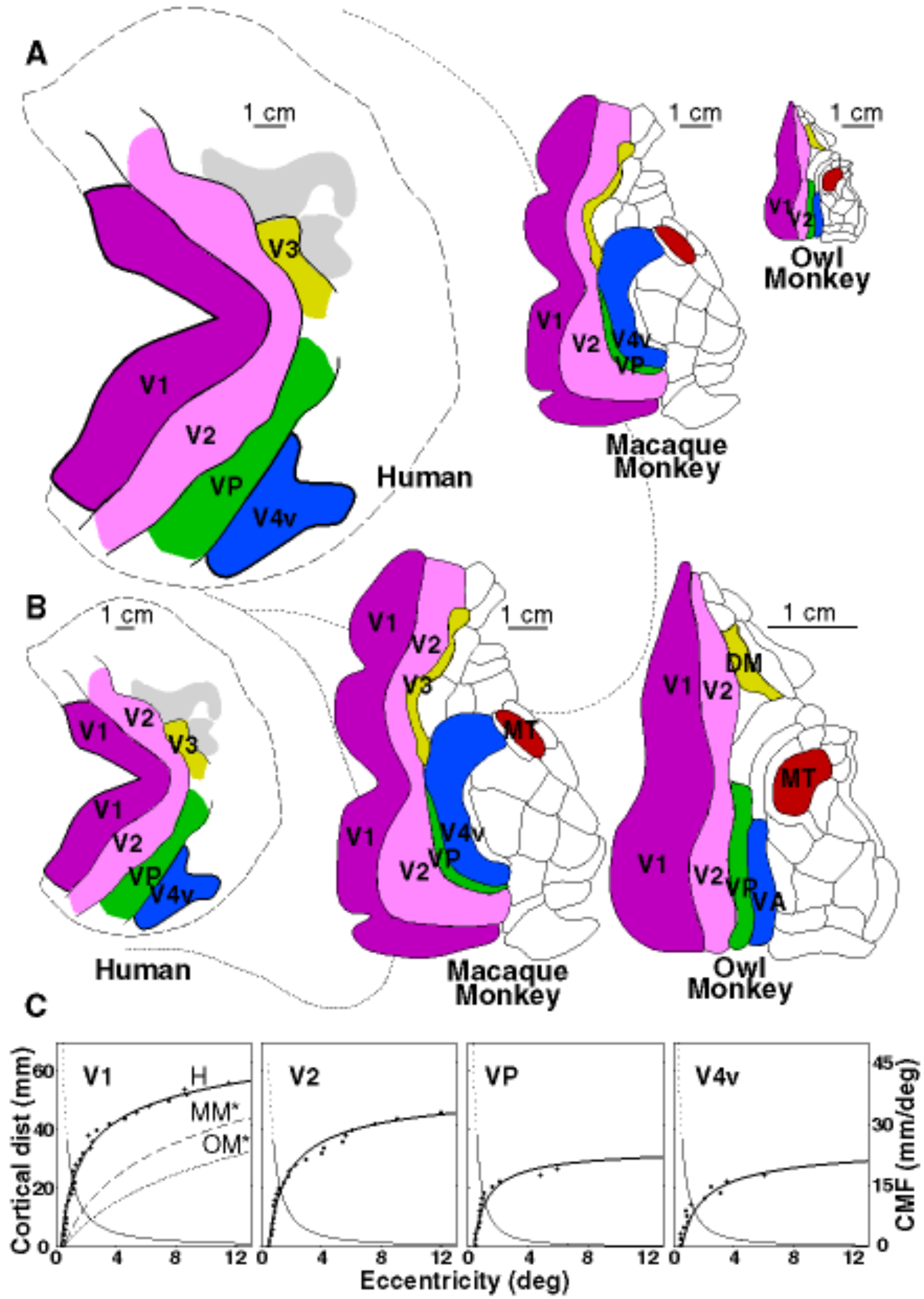

Human and macaque visual areas determined using fMRI (Brewer et al., 2002)

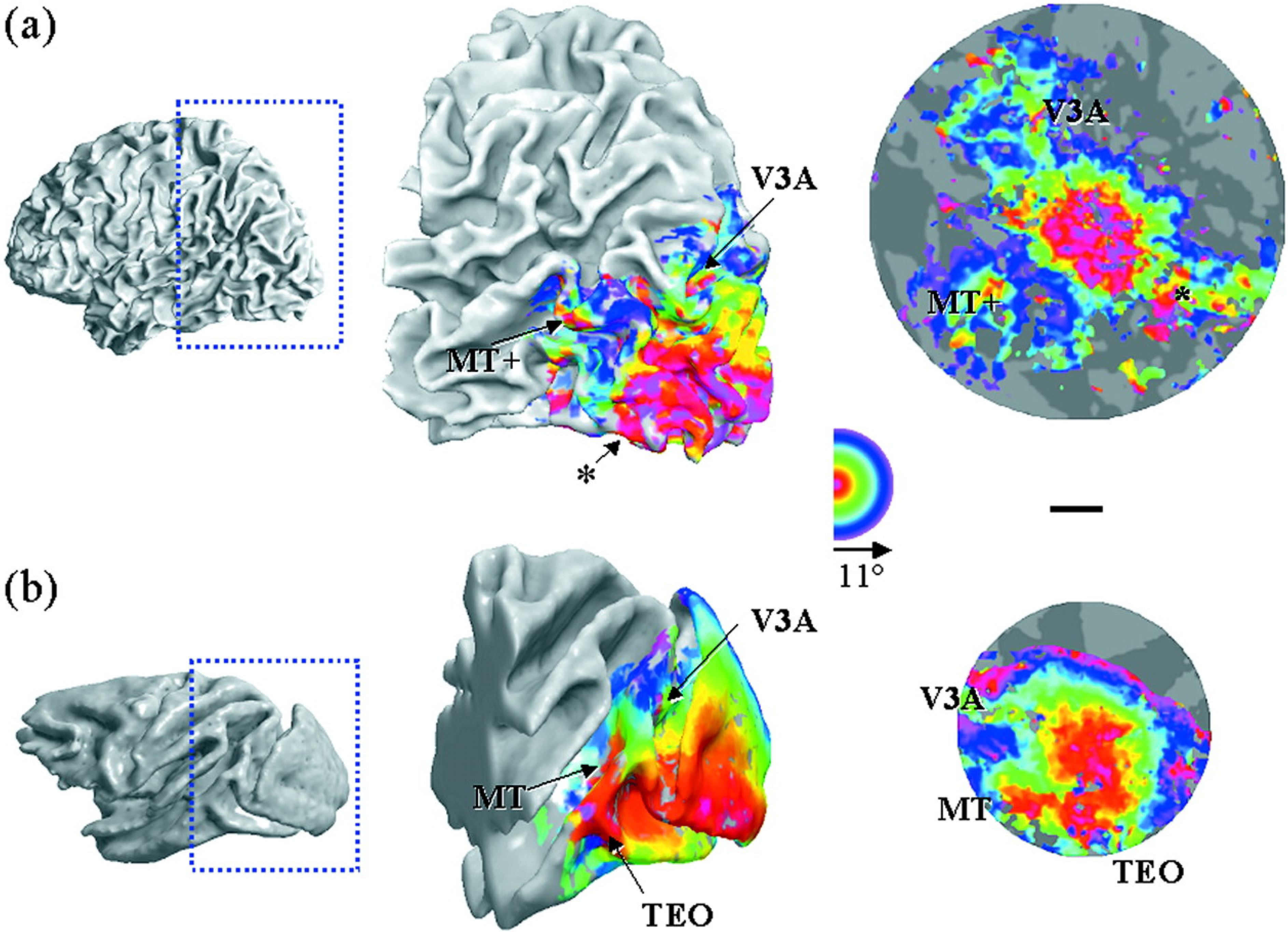

Flattening and warping the human and macaque cortex (Van Essen, 2001)

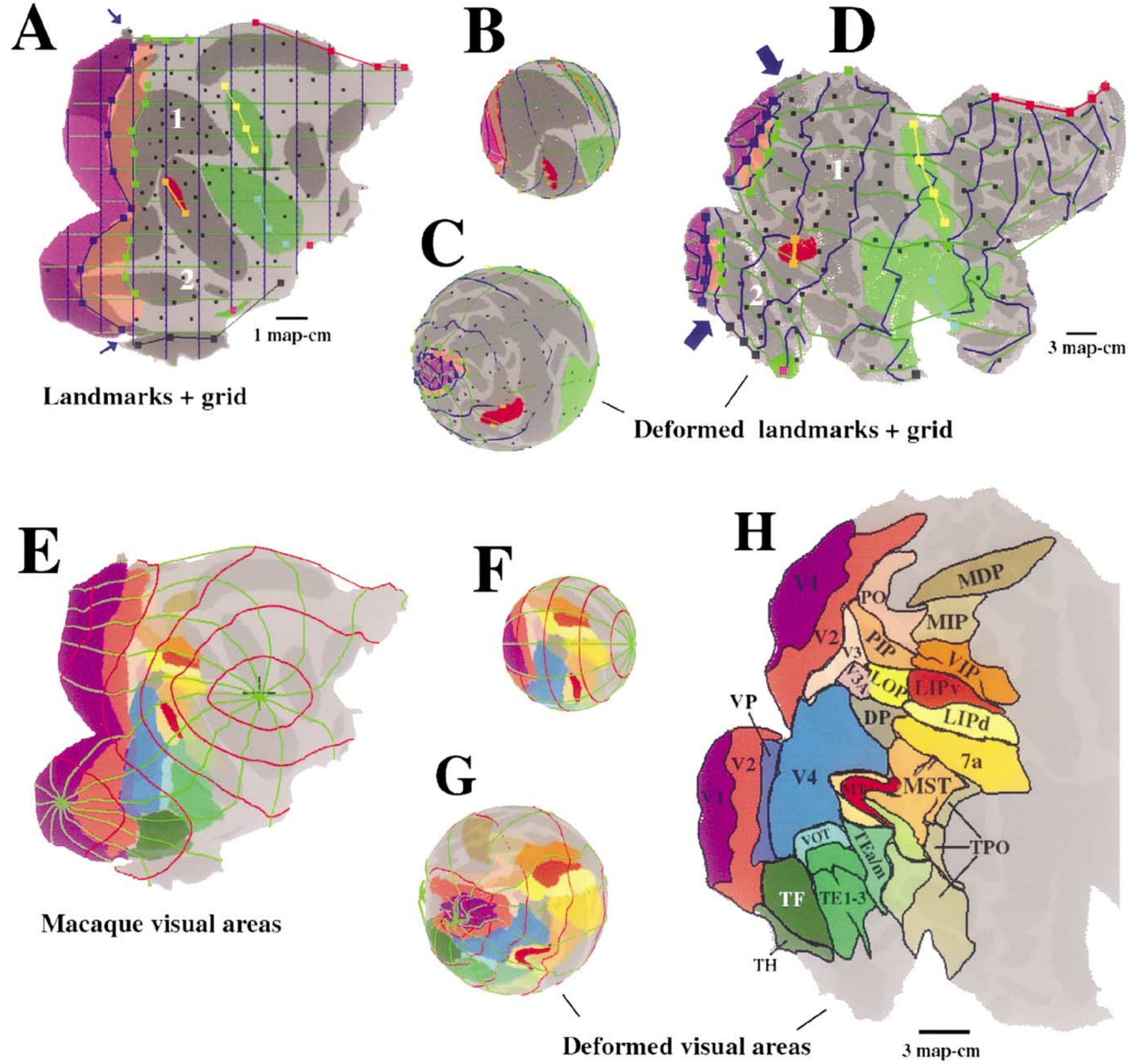

Fig. 7. Interspecies comparisons using surface-based warping from the macaque to the human map. (A) Flat map of the macaque atlas, showing landmarks used to constrain the deformation. These include areas V1, V2, MT +, the central, Sylvian, and rhinal sulci, plus landmarks on the margins of cortex along the medial wall. Grid lines were carried passively with the deformation. (B) Landmarks and grid lines projected to the macaque spherical map. (C) Landmarks and grid lines deformed to the human spherical map. Neither of the spherical maps is at the same scale as the flat maps. (D) Deformed landmarks and grid lines projected to the human flat map. (E) Visual areas on the macaque flat map, based on the Lewis and Van Essen partitioning scheme in Fig. 4, plus iso-latitude and iso-longitude lines. (F) Visual areas on the macaque spherical map, plus iso-latitude and iso-longitude lines. (G) Deformed macaque visual areas on the human spherical map, along with deformed iso-latitude and iso-longitude lines. (H) Deformed macaque visual areas on the human flat map. To download these data, connect to http://stp.wustl.edu/sums/sums.cgi?specfile = 2001-03-06-VH.R.ATLAS_DeformedMa

Human visual cortical areas

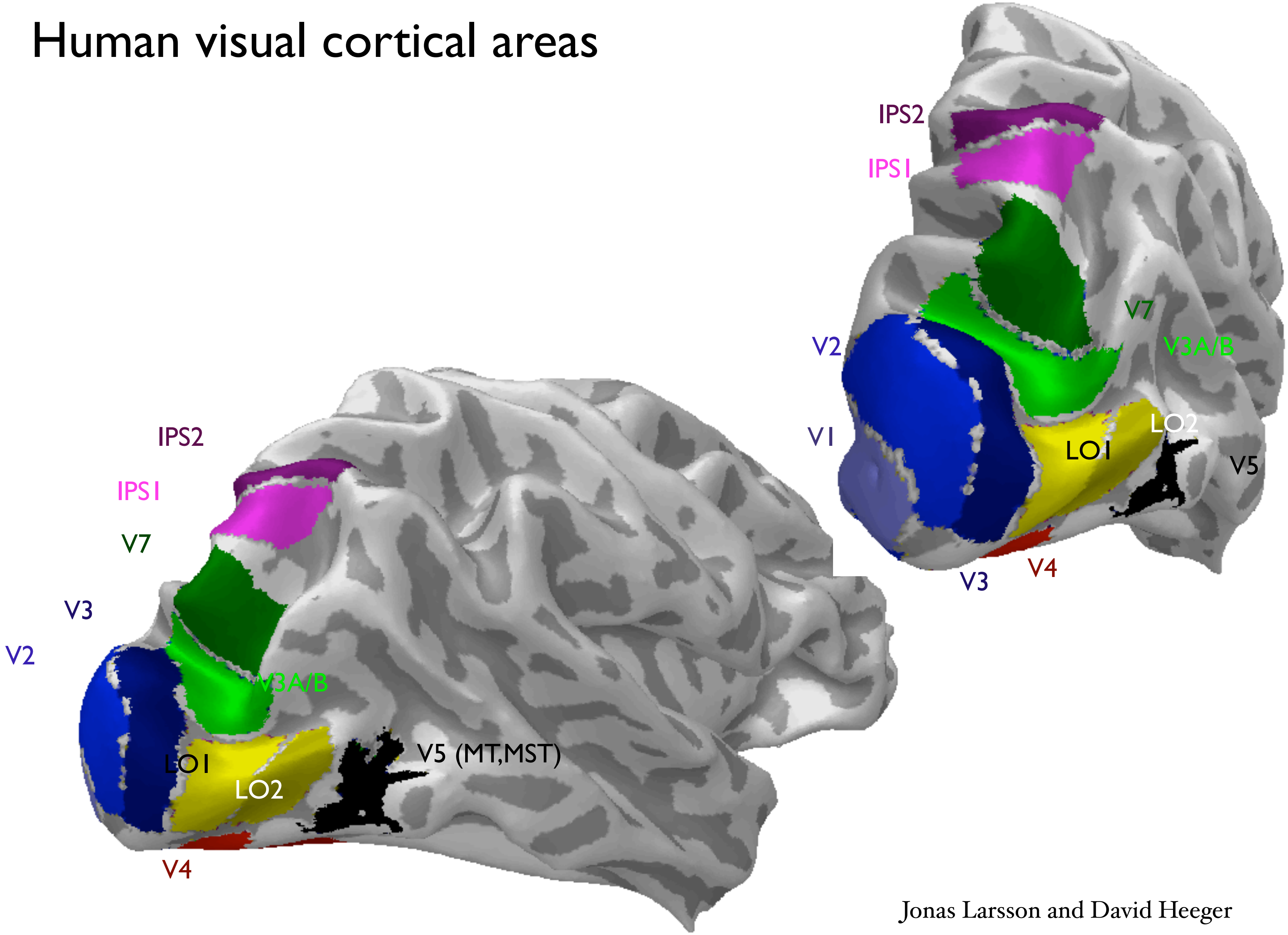

Jonas Larsson and David Heeger

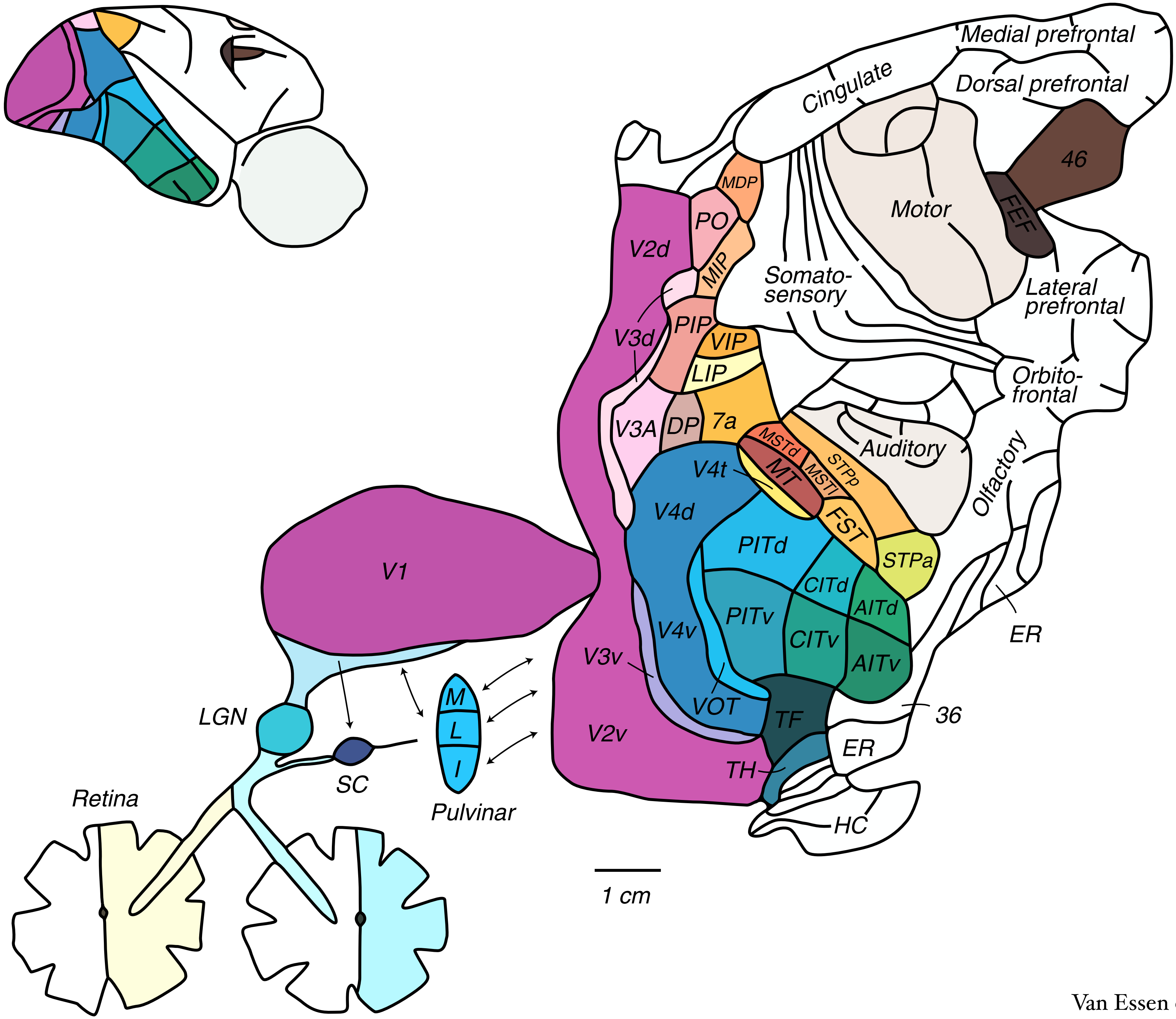

Van Essen et al., 1992

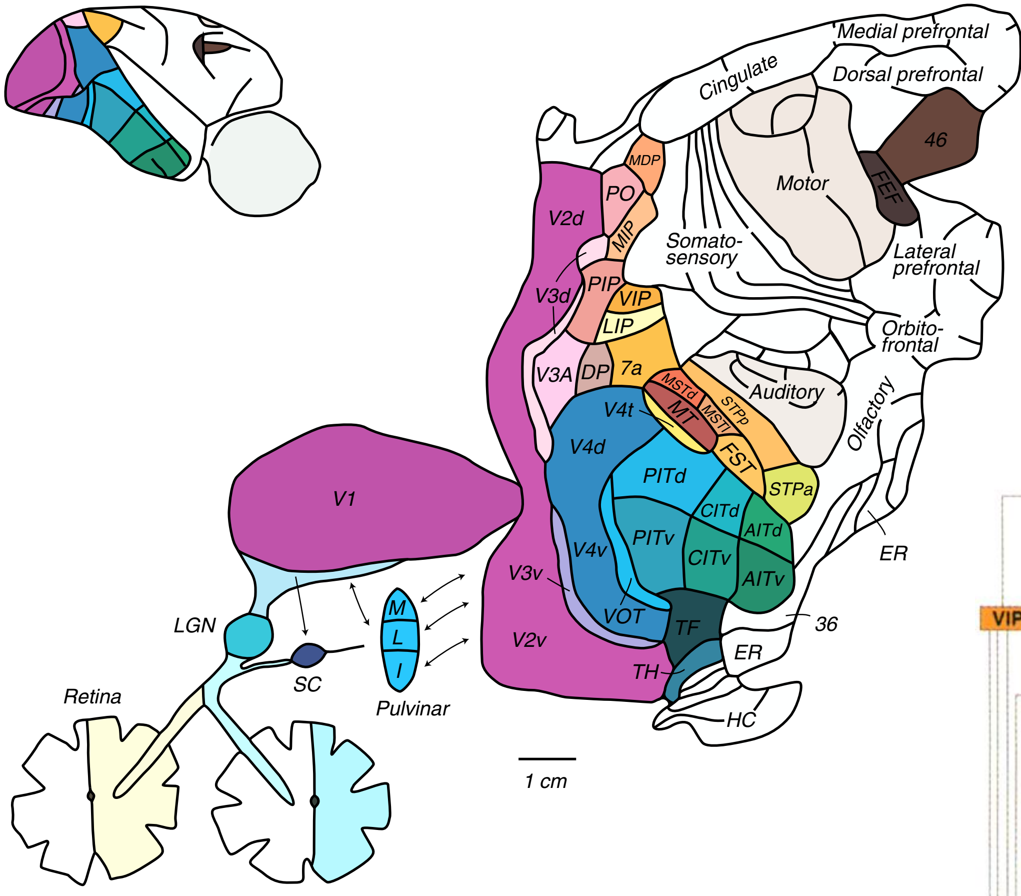

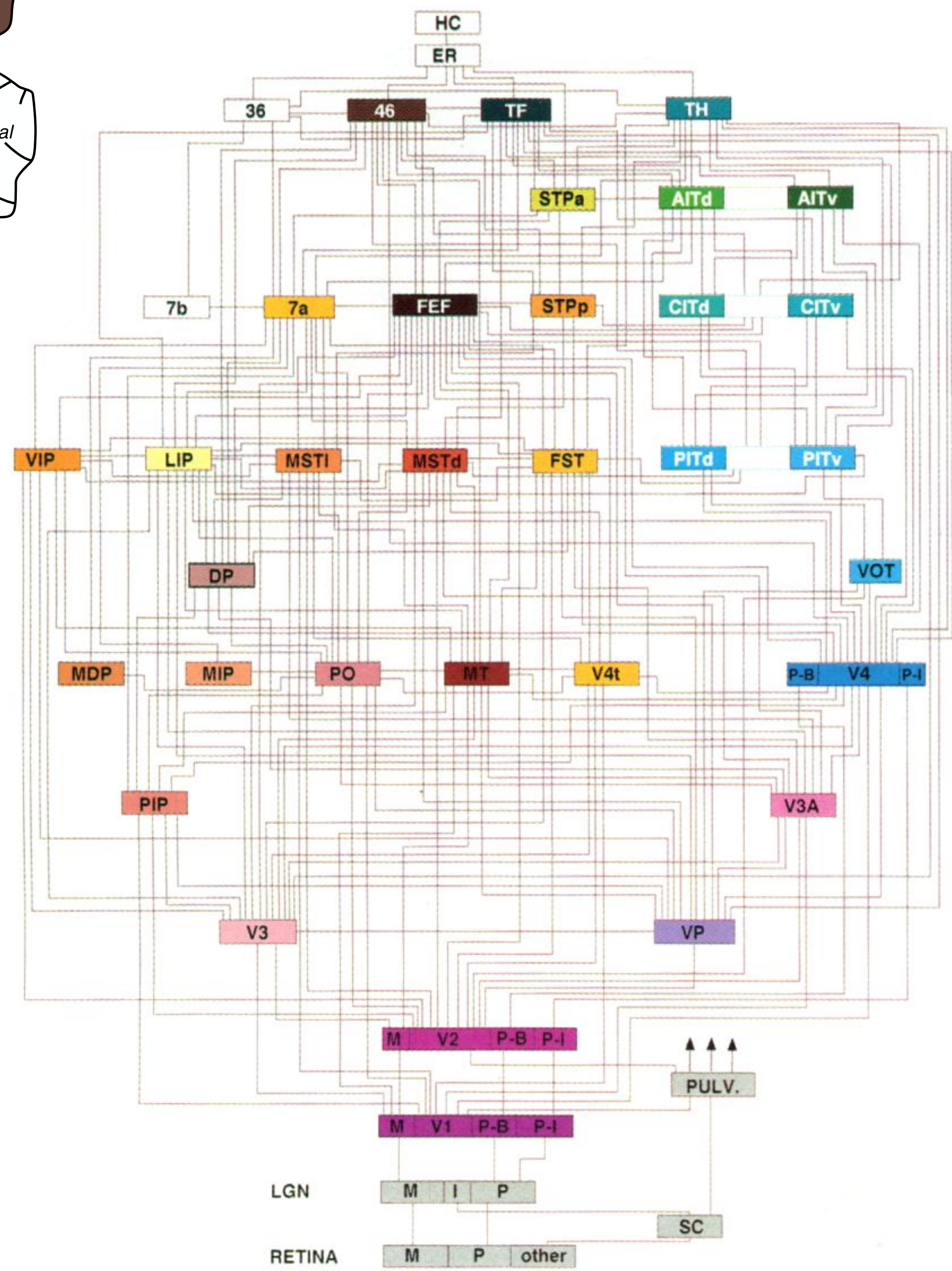

Van Essen, Anderson & Felleman, 1992

Laminar organization of cortico-cortical connections (Felleman & Van Essen, 1991; Markov et al, 2013)

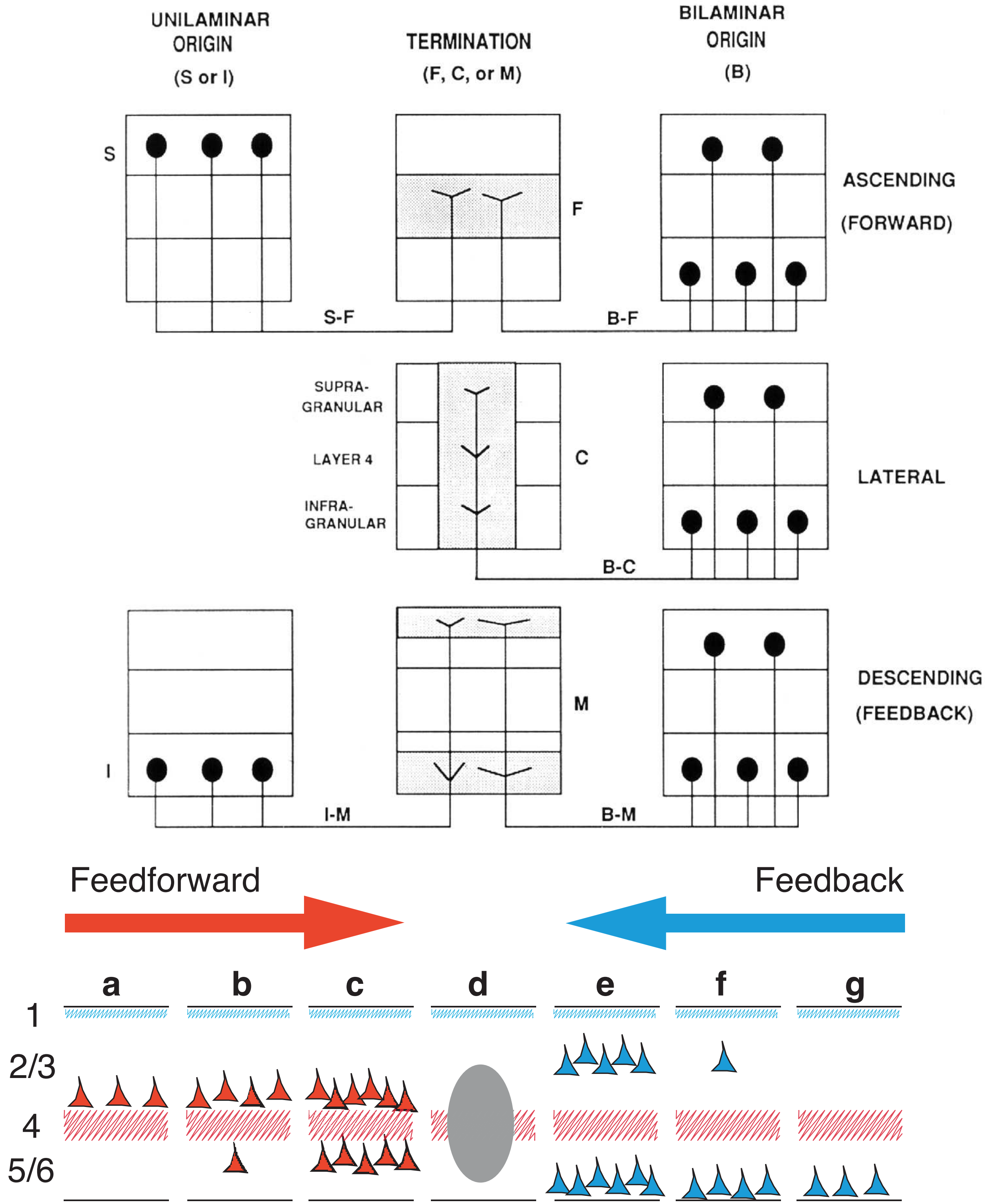

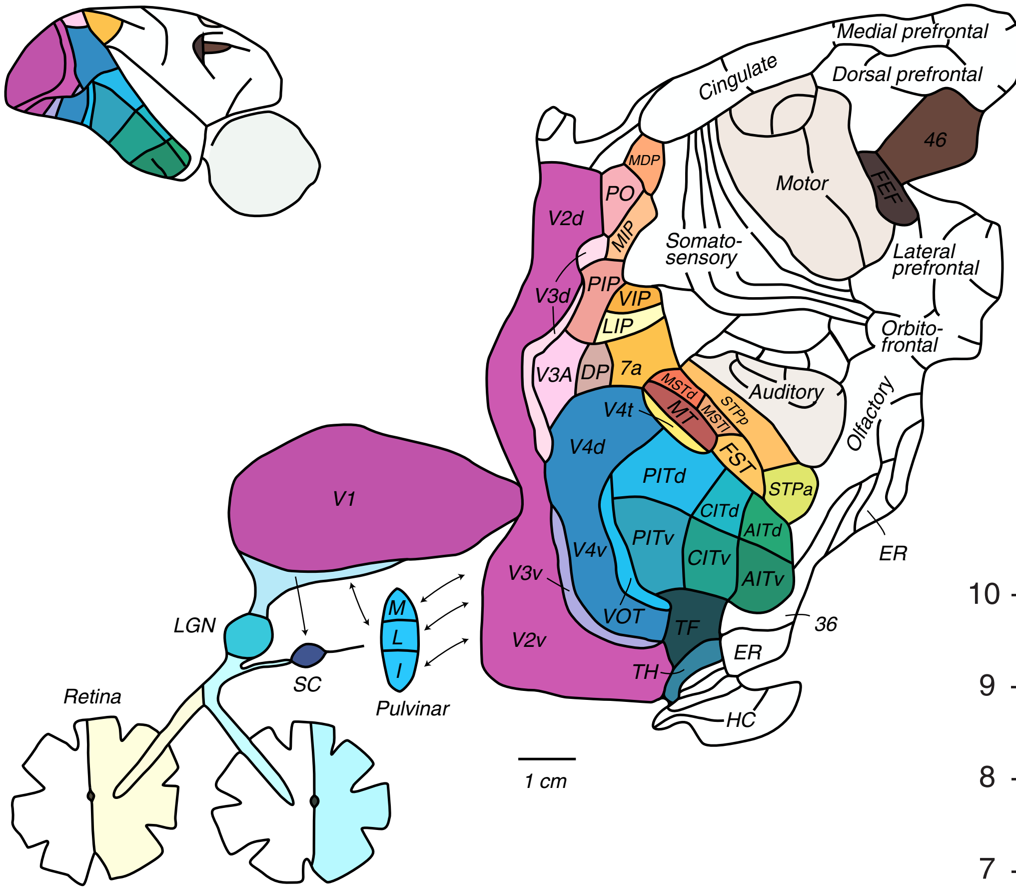

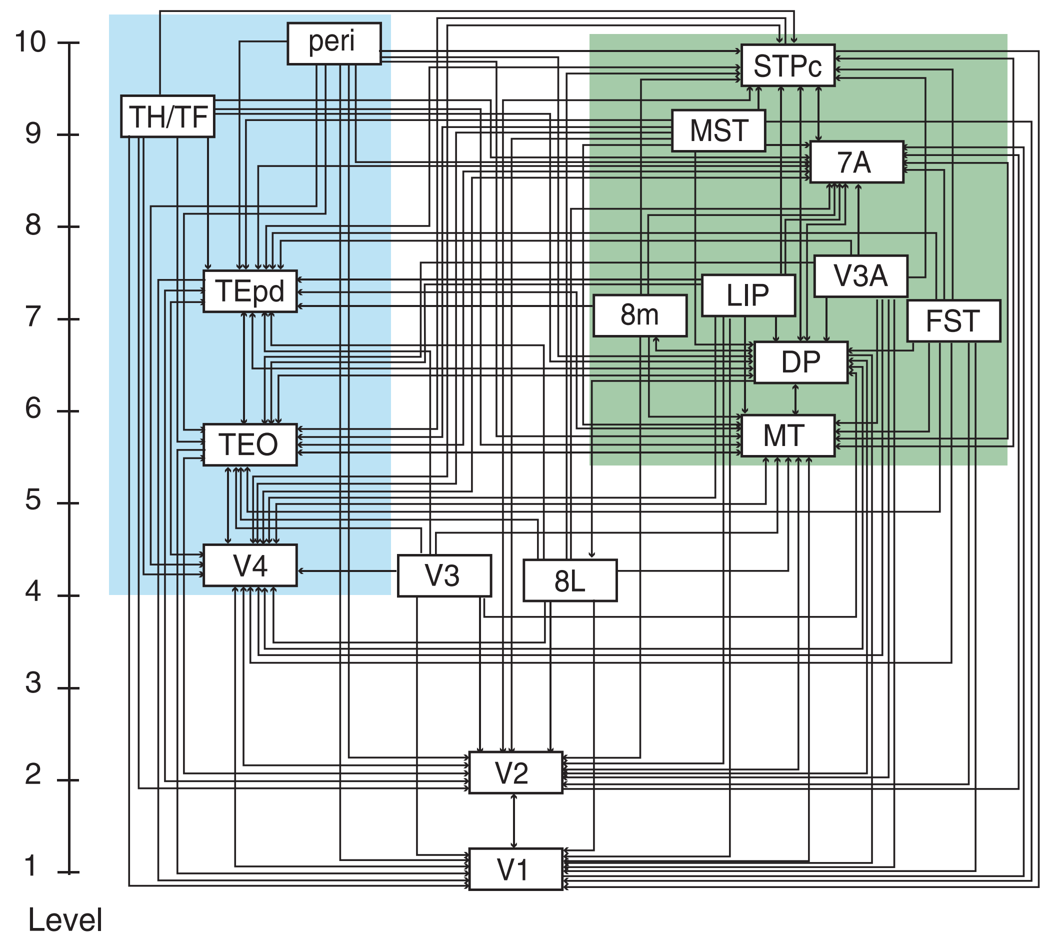

Van Essen, Anderson & Felleman, 1992; Markov et al., 2013

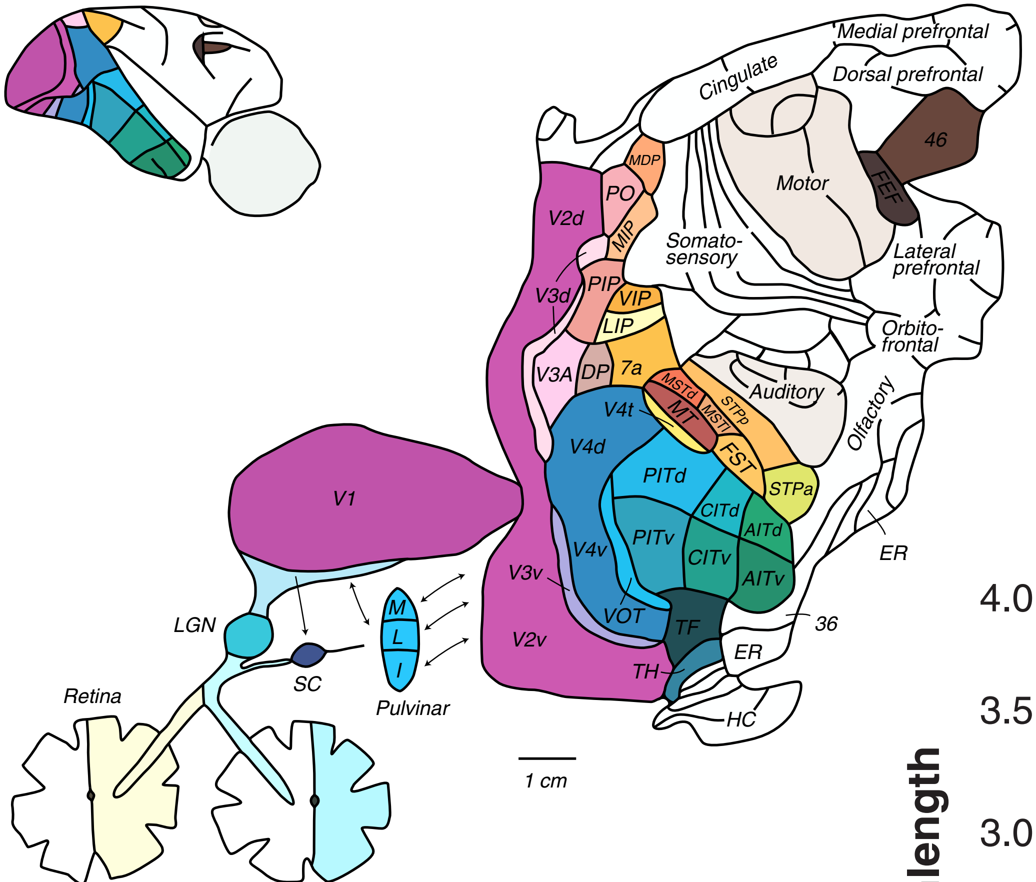

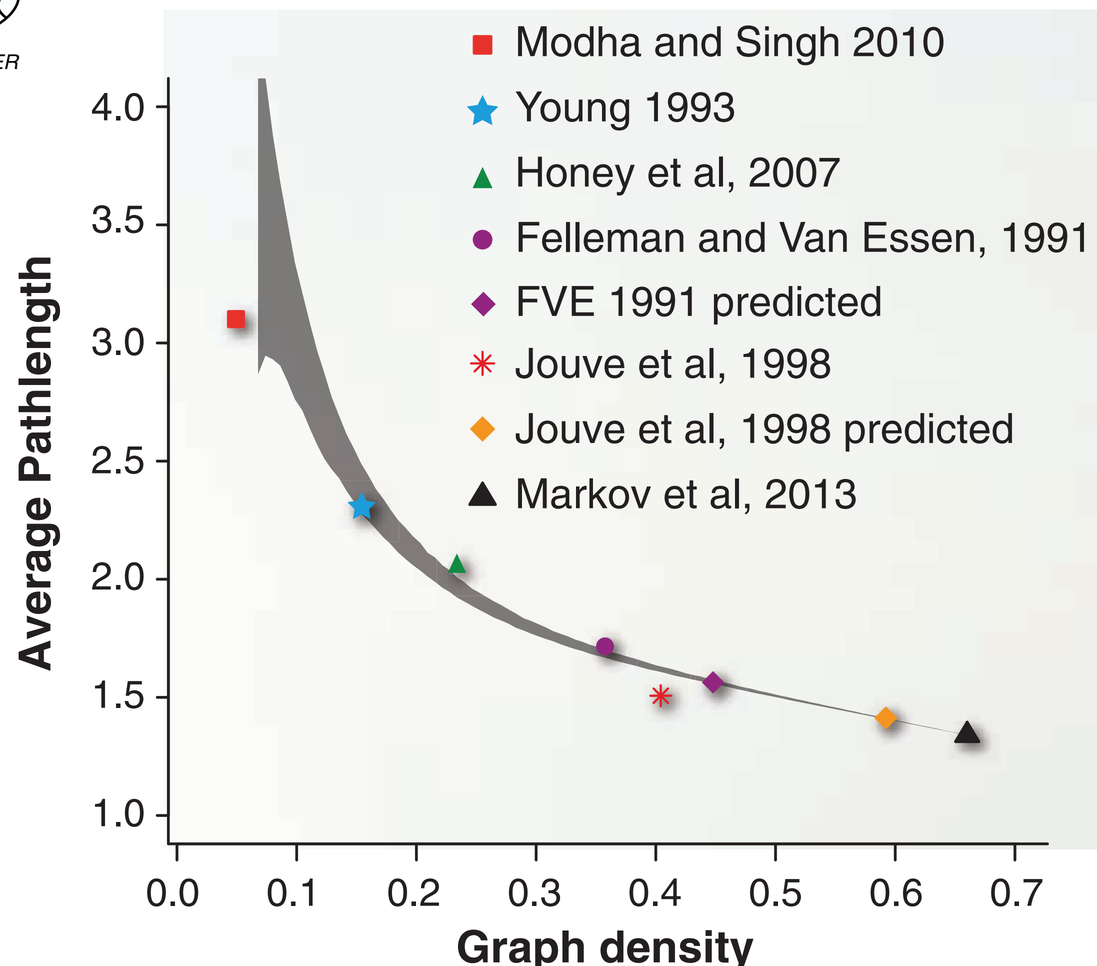

Van Essen, Anderson & Felleman, 1992; Markov et al., 2013

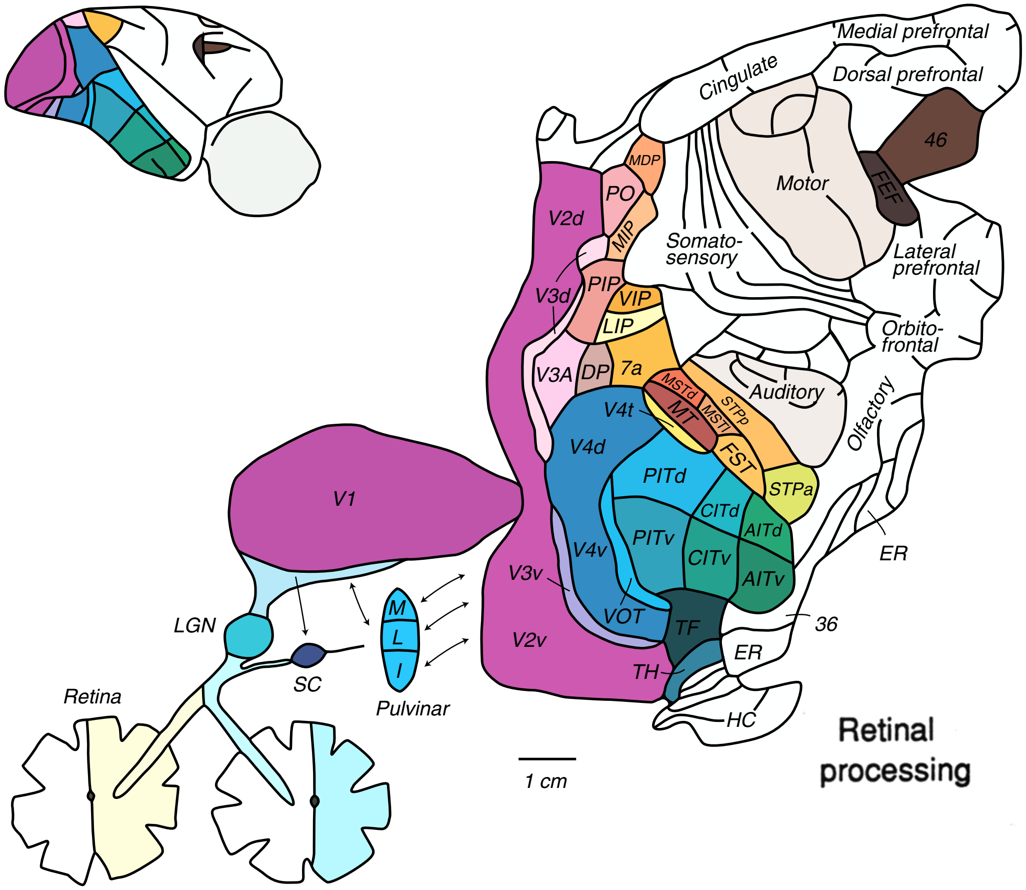

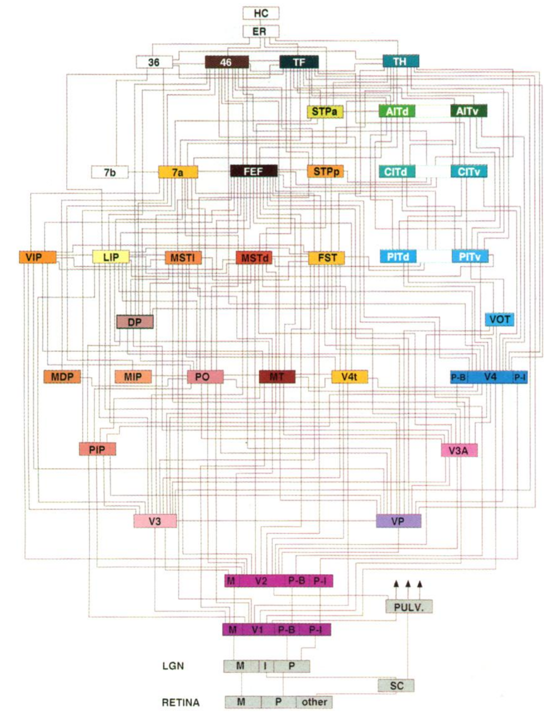

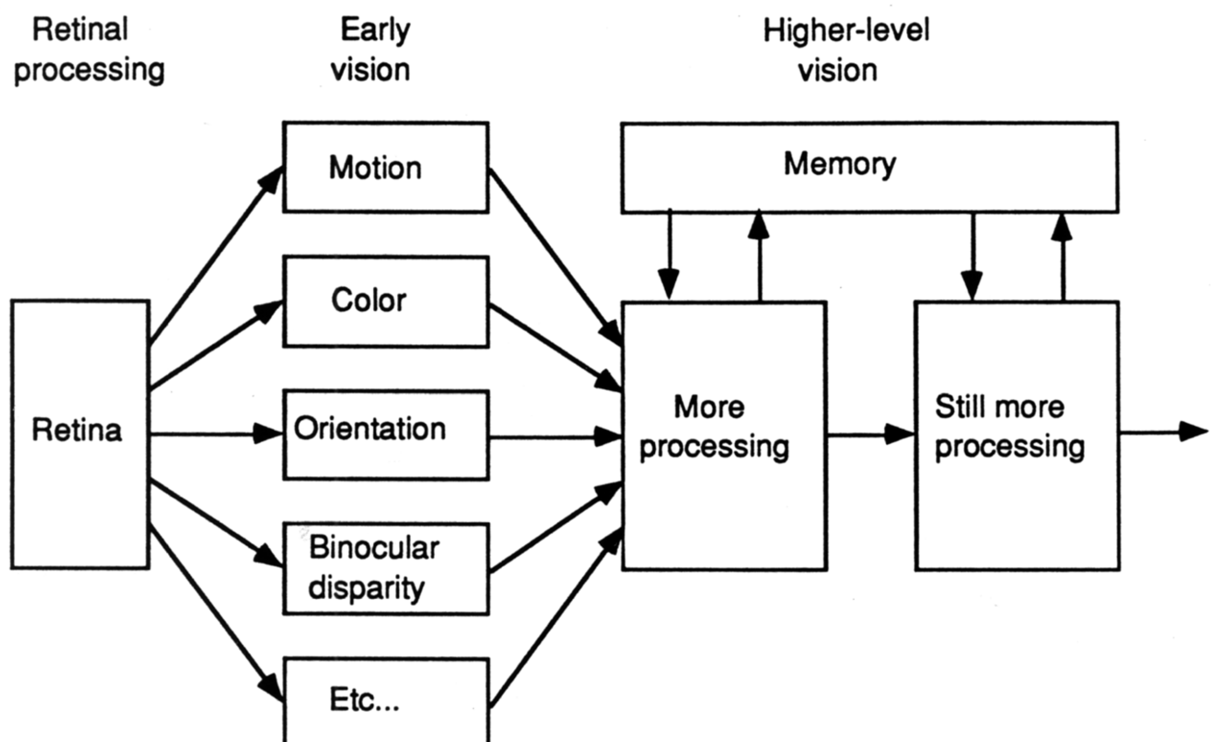

Van Essen, Anderson & Felleman, 1992

Adelson & Bergen, 1990

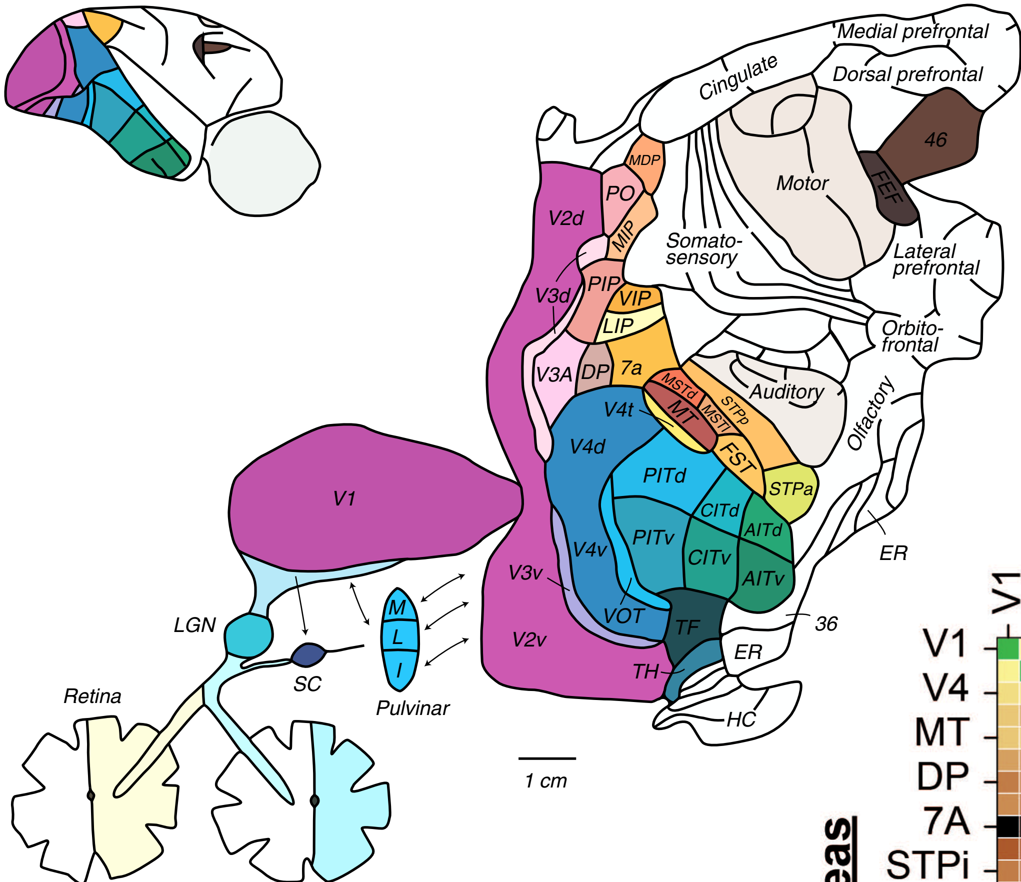

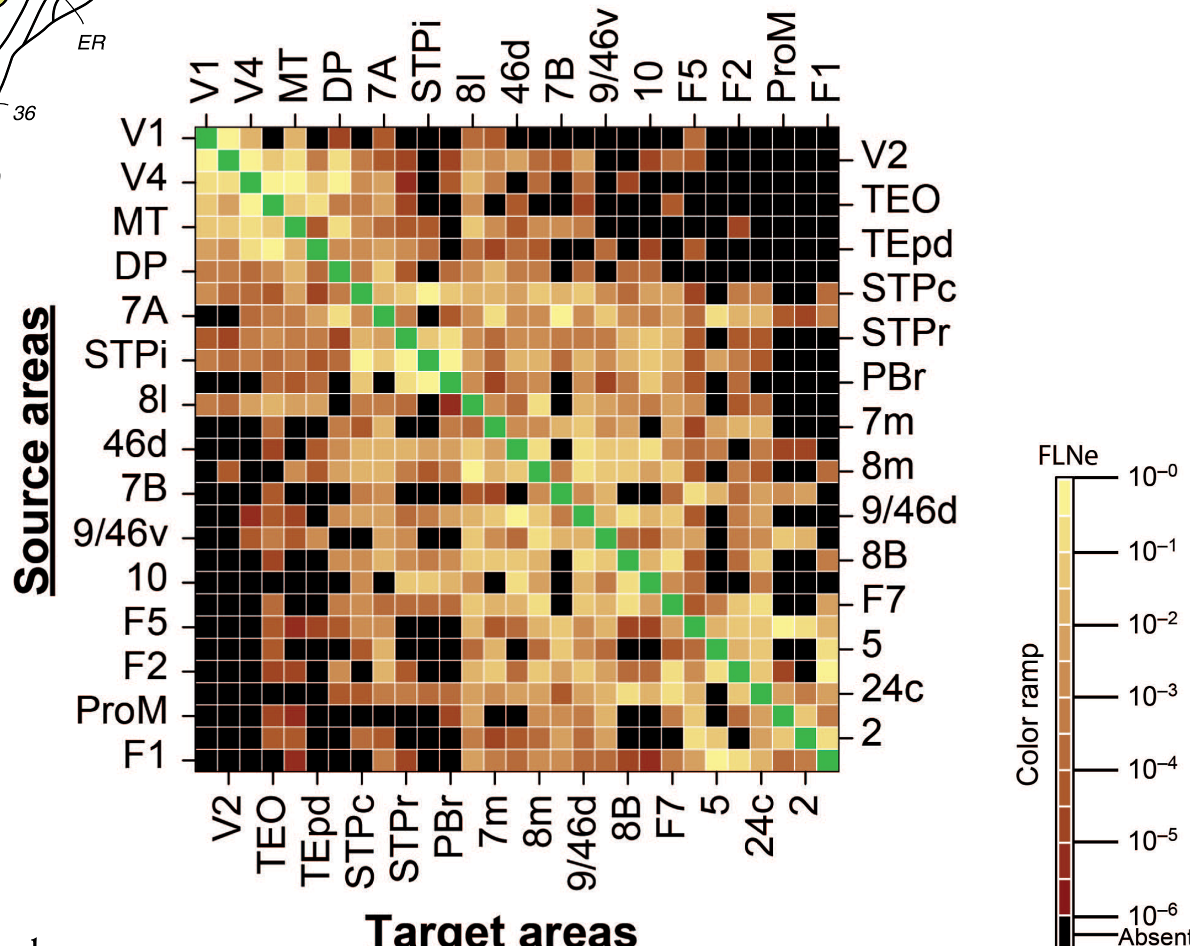

Van Essen, Anderson & Felleman, 1992; Markov et al., 2013

Extrastriate visual areas in macaque and mouse

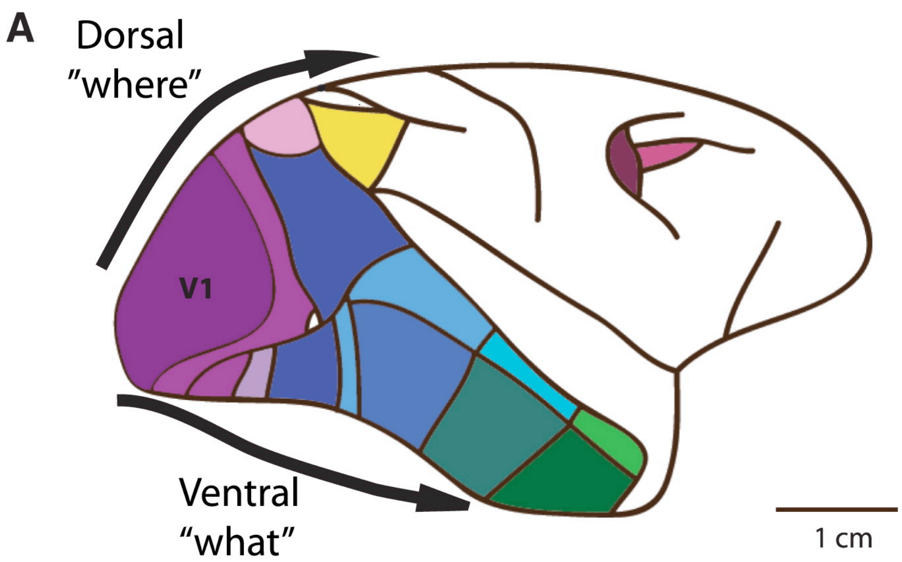

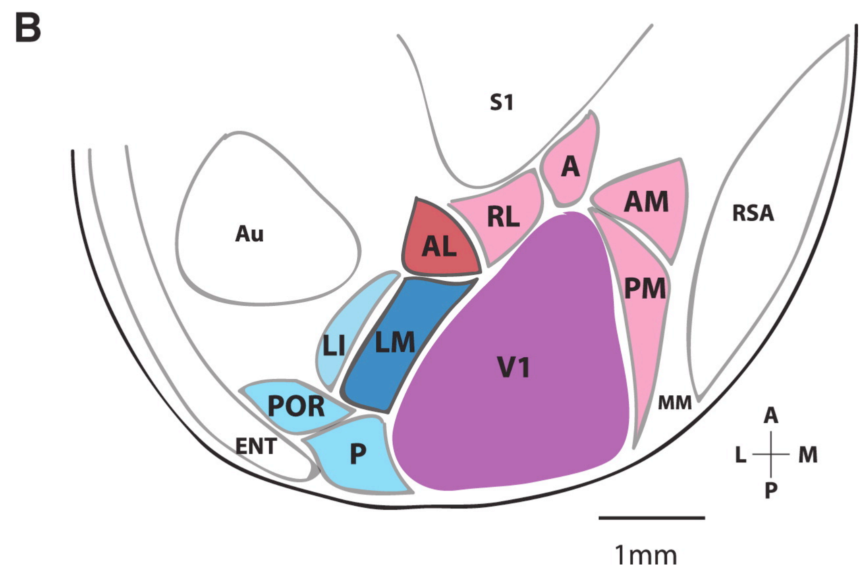

(A) Map of extrastriate cortical areas in macaque cortex. The "where" pathway extends dorsally into the parietal lobe, while the "what" pathway extends ventrally into the temporal lobe. Adapted with permission from [Felleman and Van Essen (1991)].

(B) Visual areas in mouse cortex, showing nine extrastriate areas circumscribing primary visual cortex (V1). Proposed dorsal stream and ventral stream areas are shown in red and blue, respectively, with emphasis on putative gateway areas LM and AL. Adapted with permission from [Wang and Burkhalter (2007)].

Niell, 2011

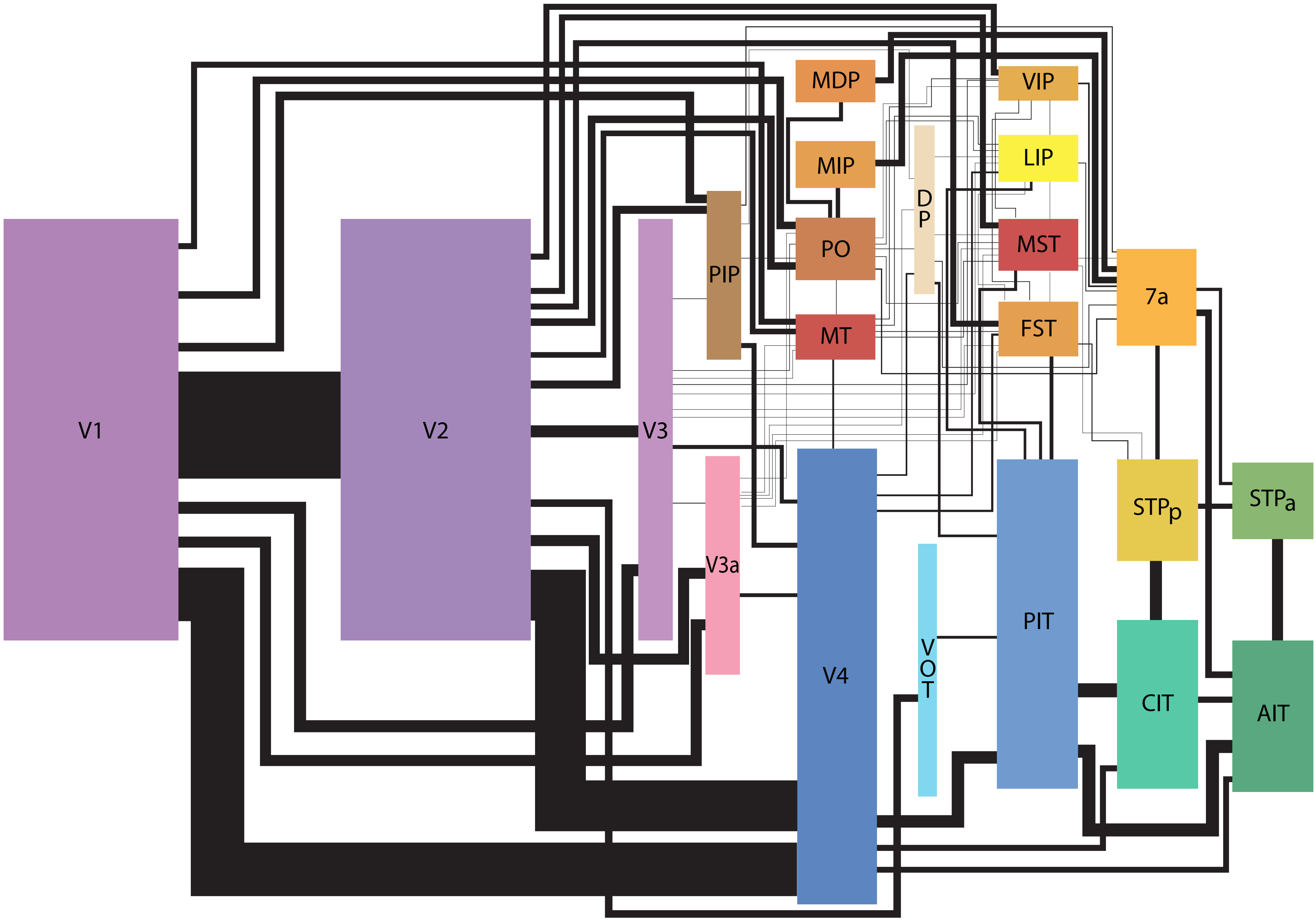

Wallisch & Movshon, 2008

after Felleman & Van Essen, 1991

Physiological evidence for parallel cortical pathways? (Felleman and Van Essen, 1987)

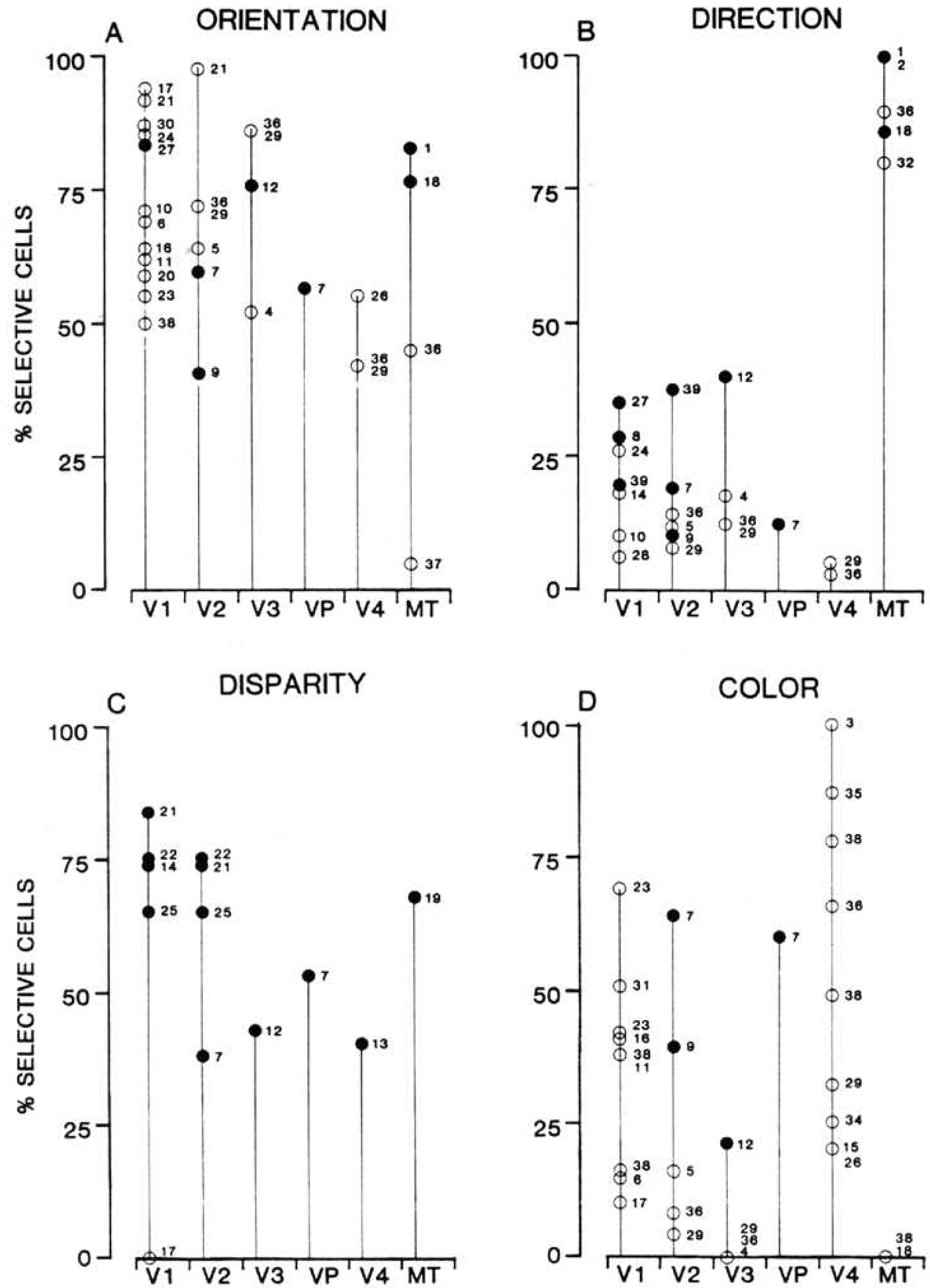

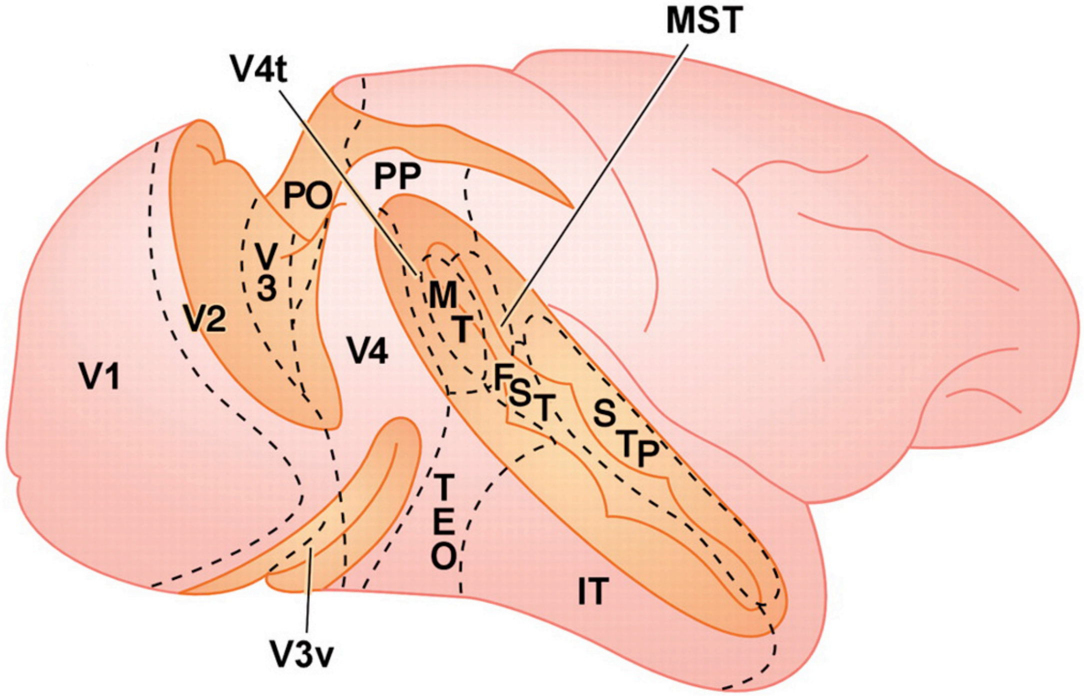

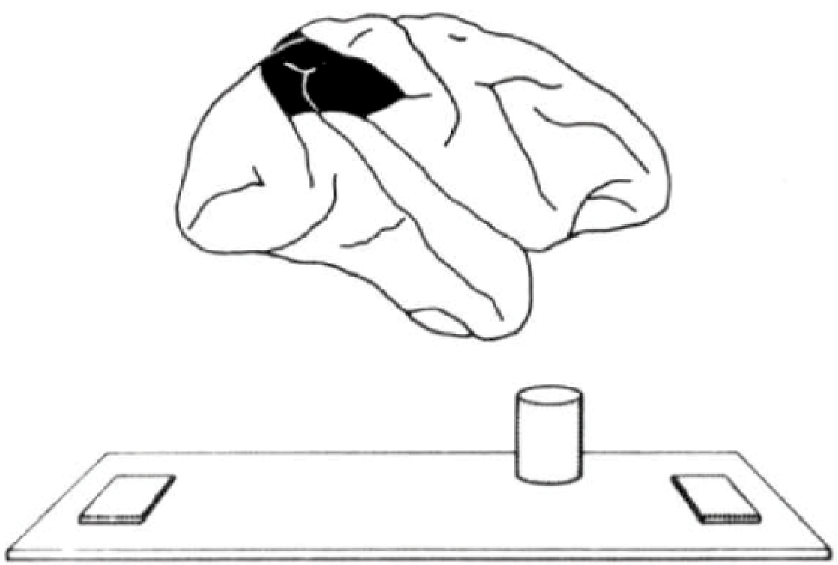

Landmark discrimination

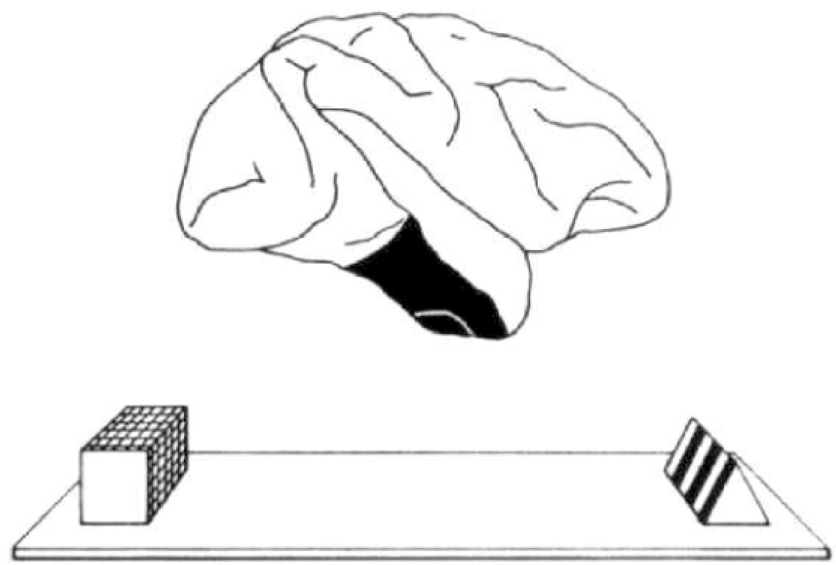

Object discrimination

Ungerleider & Mishkin, 1982

Sir David Ferrier

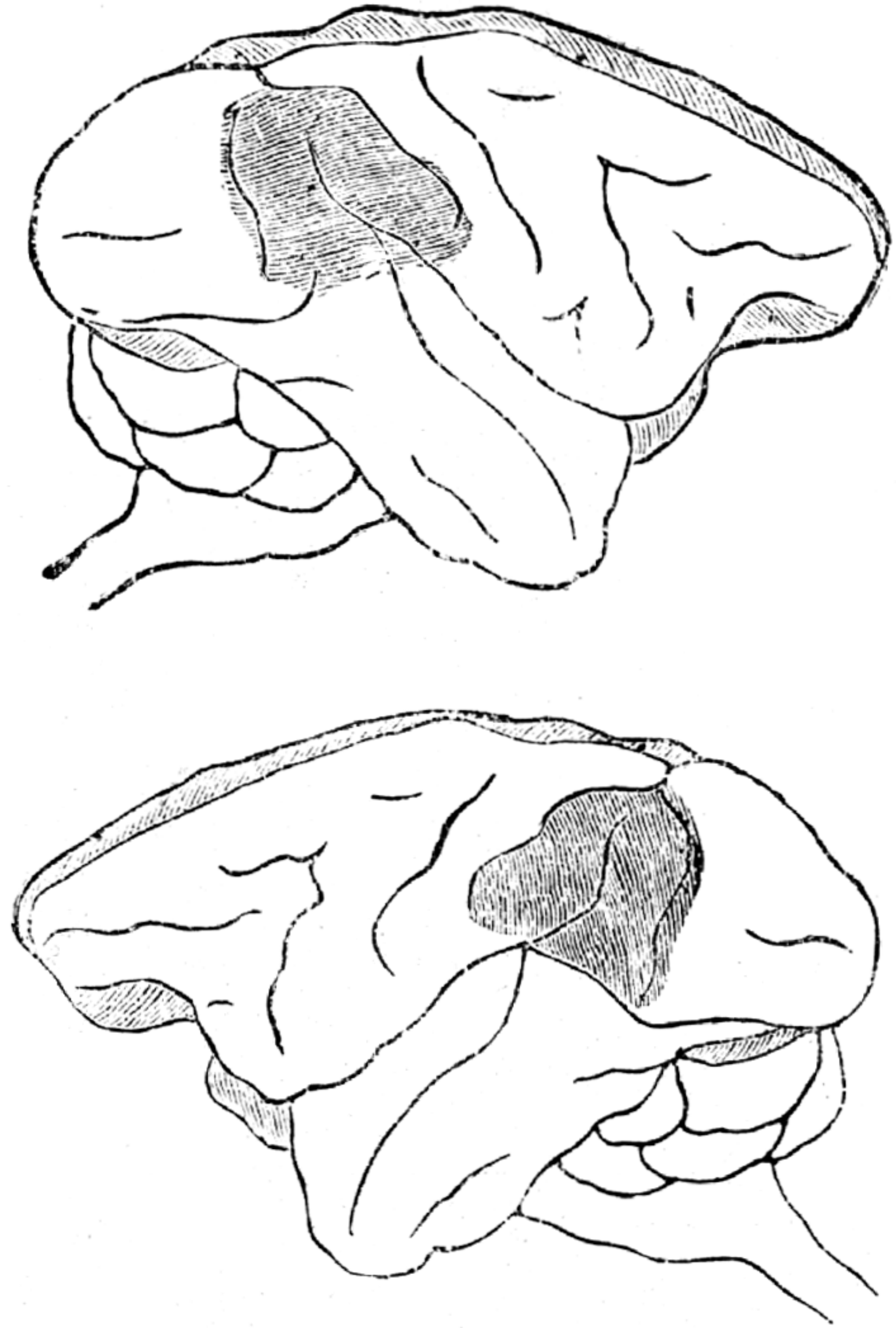

Lesions that caused blindness

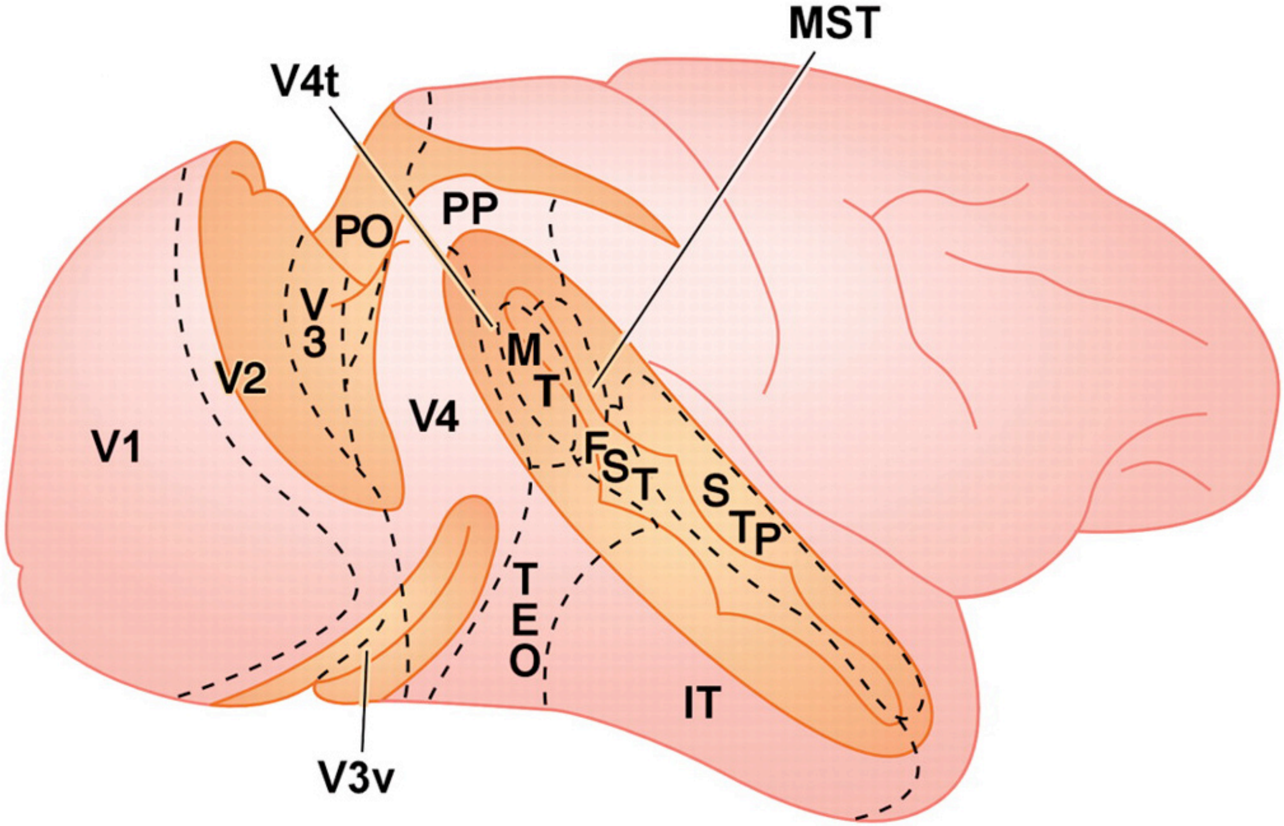

Dorsal pathway
Space, motion, action

Ventral pathway
Form, recognition, memory

Ungerleider & Mishkin, 1982

Functional specialization in human extrastriate visual cortex

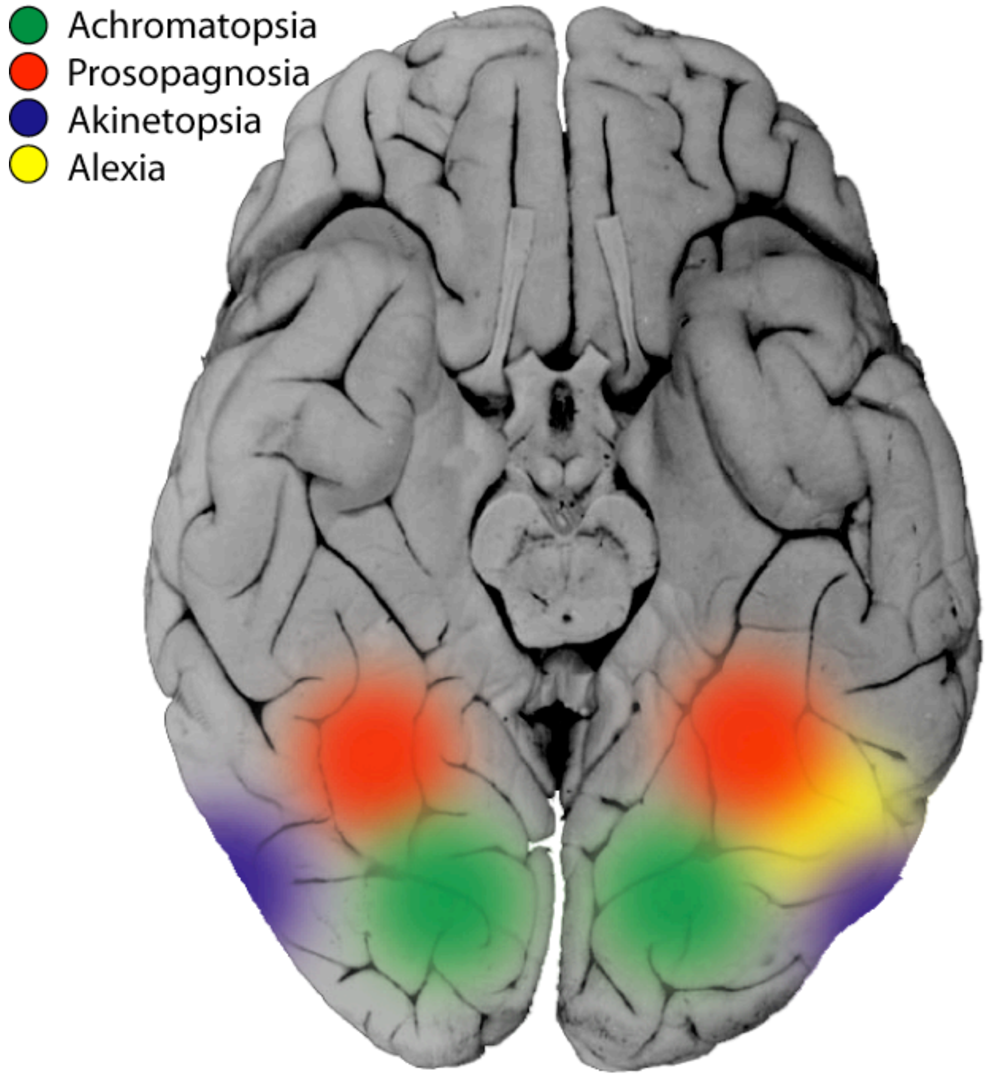

Dissociating vision for perception and vision for action

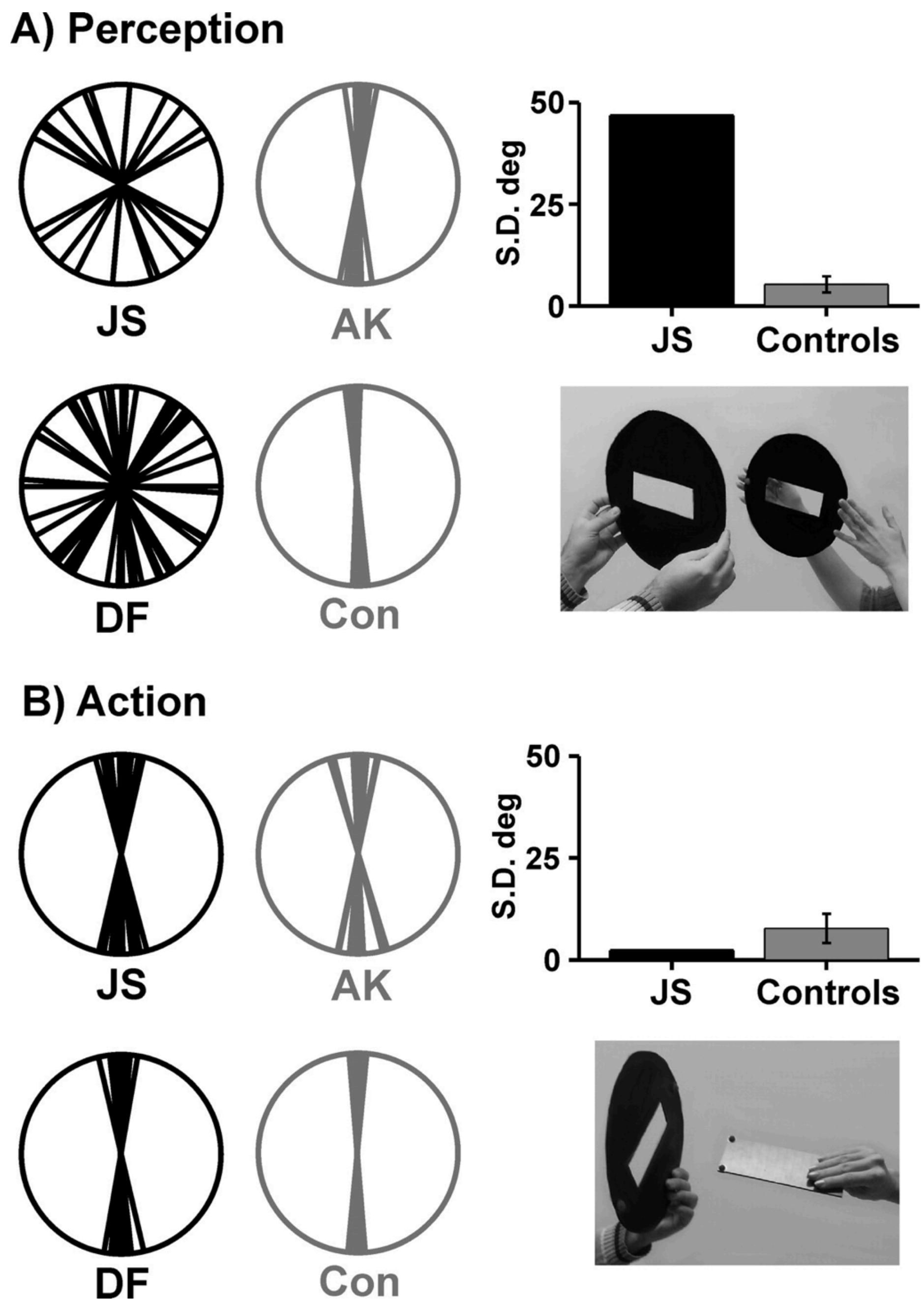

Polar plots illustrating perceptual orientation judgements (***A***) and orientation adaptation in reaching movements (***B***). The photo inlays illustrate the respective tasks. The different orientations of individual trials have been normalized to the vertical. The polar plots therefore show difference values to the vertical, representing a difference to the target orientation of 0°. Black data plots indicate the data of our patient J.S. and the data of VFA patient D.F. reported by Milner and Goodale (1995). Gray polar plots indicate an exemplary control of our study (A.K.) and the control subject reported by Milner and Goodale (1995) (Con). Bar plots illustrate SDs of J.S.'s responses in either task and average SDs in our group of healthy controls (error bars denote 1 SD).

Milner & Goodale, 1995; Karnath et al 2009

Dissociating vision for perception and vision for action

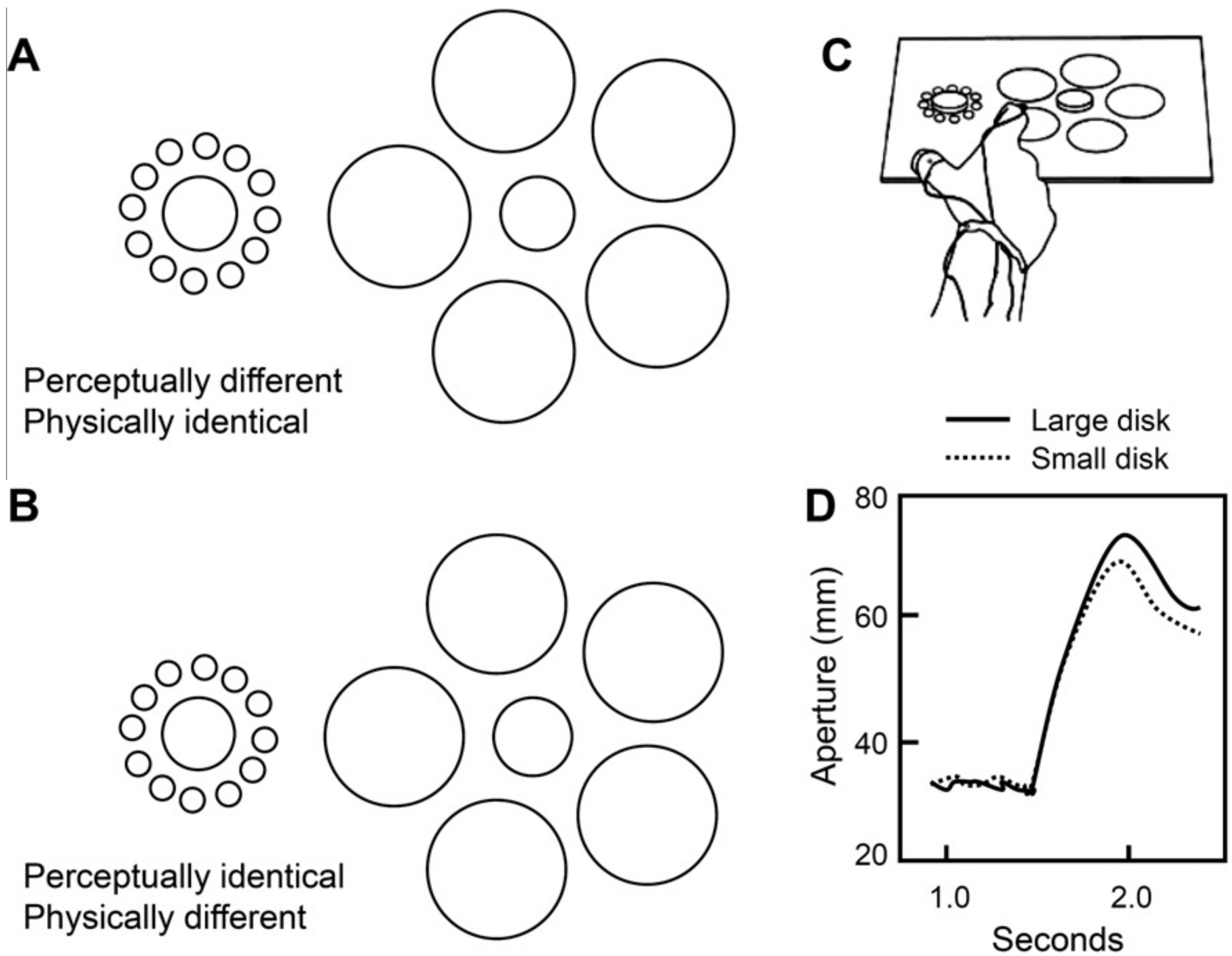

Fig. 7. The effect of a size-contrast illusion on perception and action. (A) The traditional Ebbinghaus illusion in which the central circle in the annulus of larger circles is typically seen as smaller than the central circle in the annulus of smaller circles, even though both central circles are actually the same size. (B) The same display, except that the central circle in the annulus of larger circles has been made slightly larger. As a consequence, the two central circles now appear to be the same size. (C) A 3-D version of the Ebbinghaus illusion. Participants are instructed to pick up one of the two 3-D disks placed either on the display shown in Panel A or the display shown in Panel B. (D) Two trials with the display shown in Panel B, in which the participant picked up the small disk on one trial and the large disk on another. Even though the two central disks were perceived as being the same size, the grip aperture in flight reflected the real not the apparent size of the disks. Adapted with permission from Aglioti et al. (1995).

Goodale, 2010

Single stream lesion

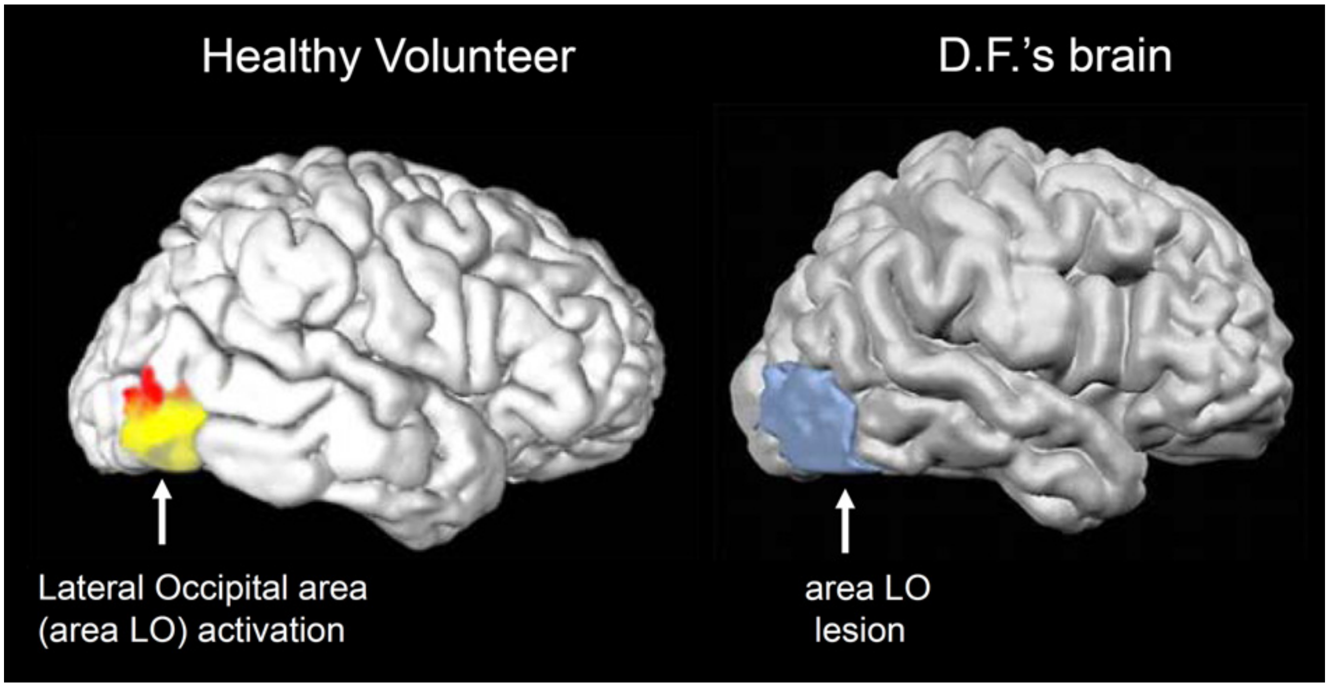

Fig. 3. Area LO, a ventral-stream area implicated in object recognition (particularly object form), has been localized on the brain of a healthy control subject by comparing fMRI activation to intact versus scrambled line drawings. Note that the lesion (marked in blue) on patient D.F.'s right cerebral hemisphere encompasses all of area LO. Area LO in D.F.'s left hemisphere is also completely damaged. Adapted with permission from Goodale and Milner (2004).

Goodale, 2010

Dissociating vision for perception and vision for action

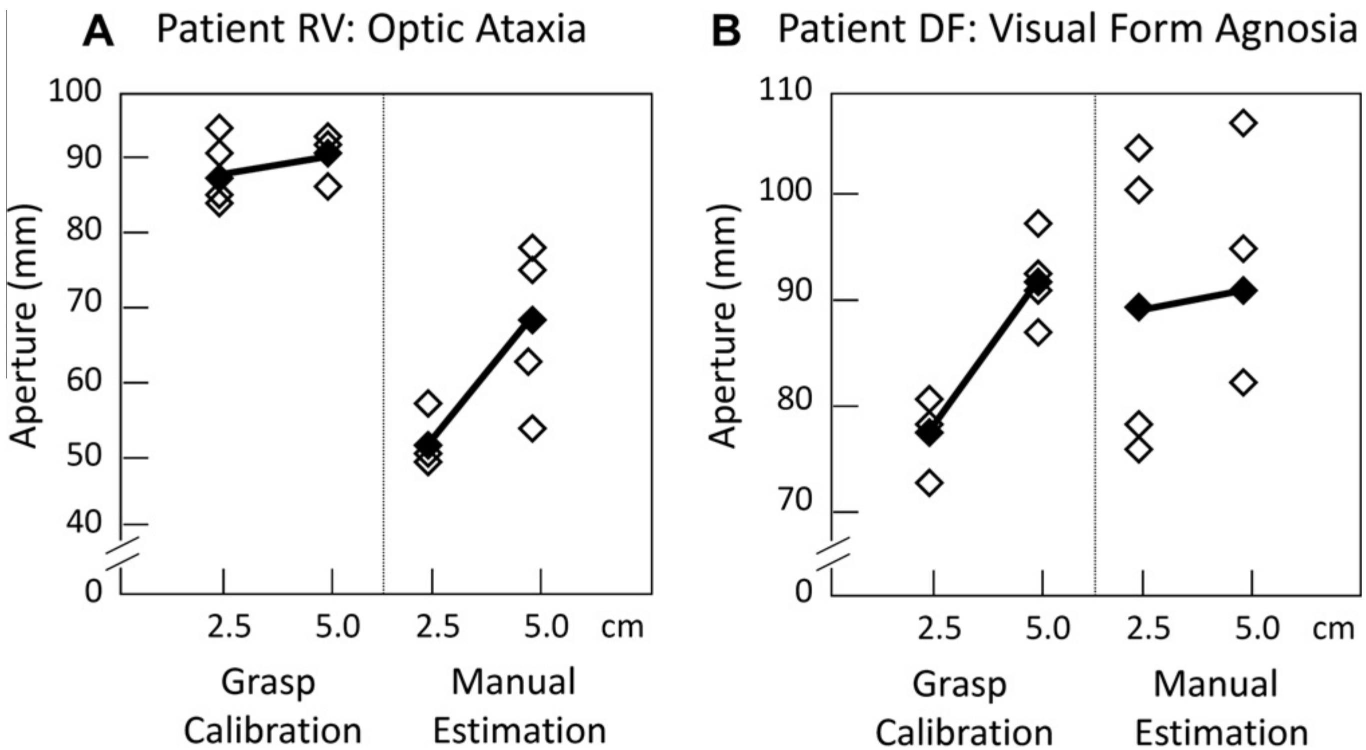

Fig. 2. Graphs showing the size of the aperture between the index finger and thumb during object-directed grasping and manual estimates of object width for RV, a patient with optic ataxia, and DF, a patient with visual form agnosia. Panel A shows that RV was able to indicate the size of the objects reasonably well (individual trials marked as open diamonds), but her maximum grip aperture in flight was not well-tuned. She simply opened her hand as wide as possible on every trial. In contrast, Panel B shows that DF showed excellent grip scaling, opening her hand wider for the 50 mm-wide object than for the 25-mm wide object. D.F.'s manual estimates of the width of the two objects, however, were grossly inaccurate and showed enormous variability from trial to trial.

Goodale, 2010

Monkey Visual Areas


Adapted from Motter and Mountcastle 1981

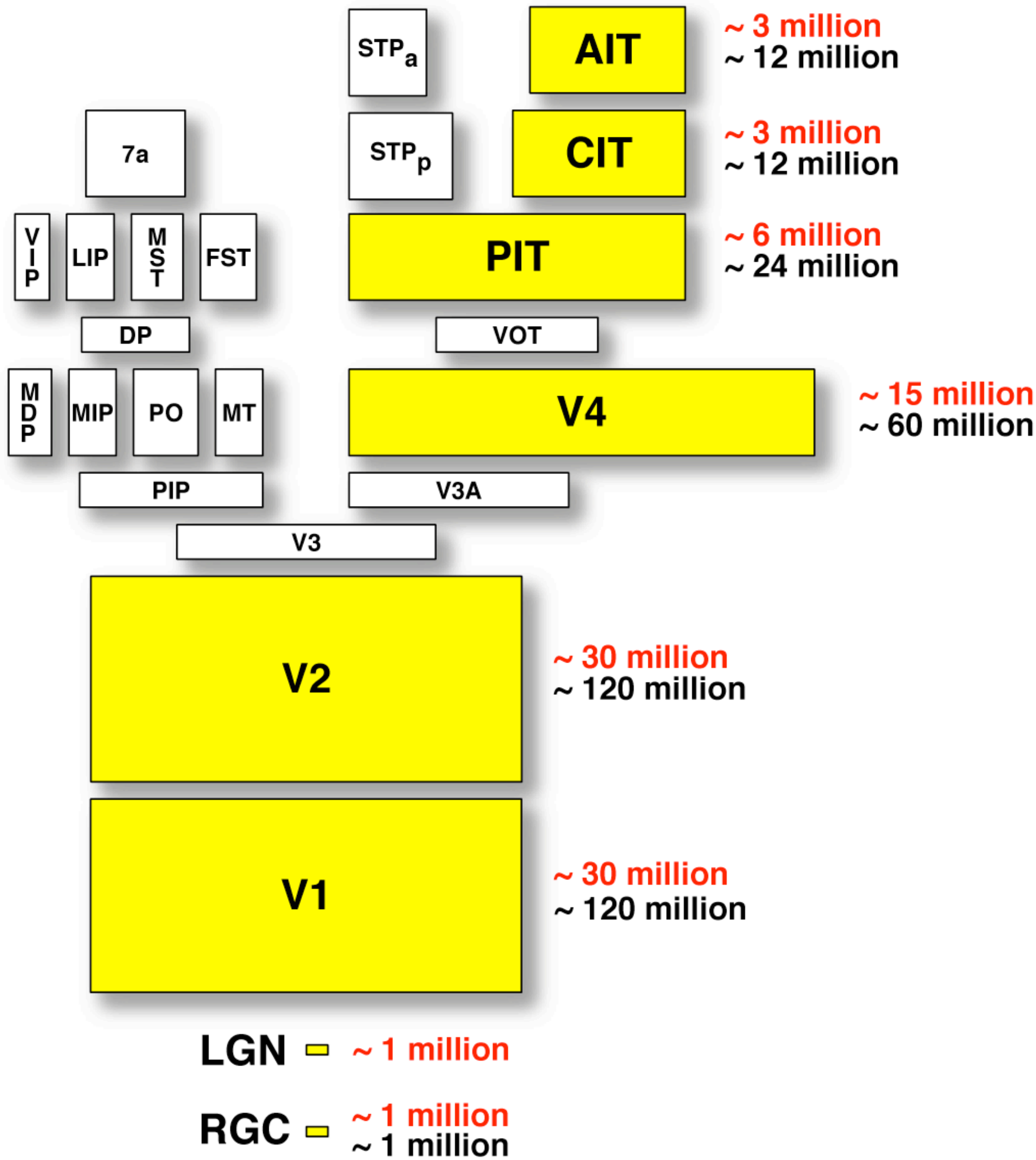

Total number of neurons

Total number of feedforward projection neurons

(both hemispheres)

Adapted from John Maunsell

Speed of processing in the ventral pathway

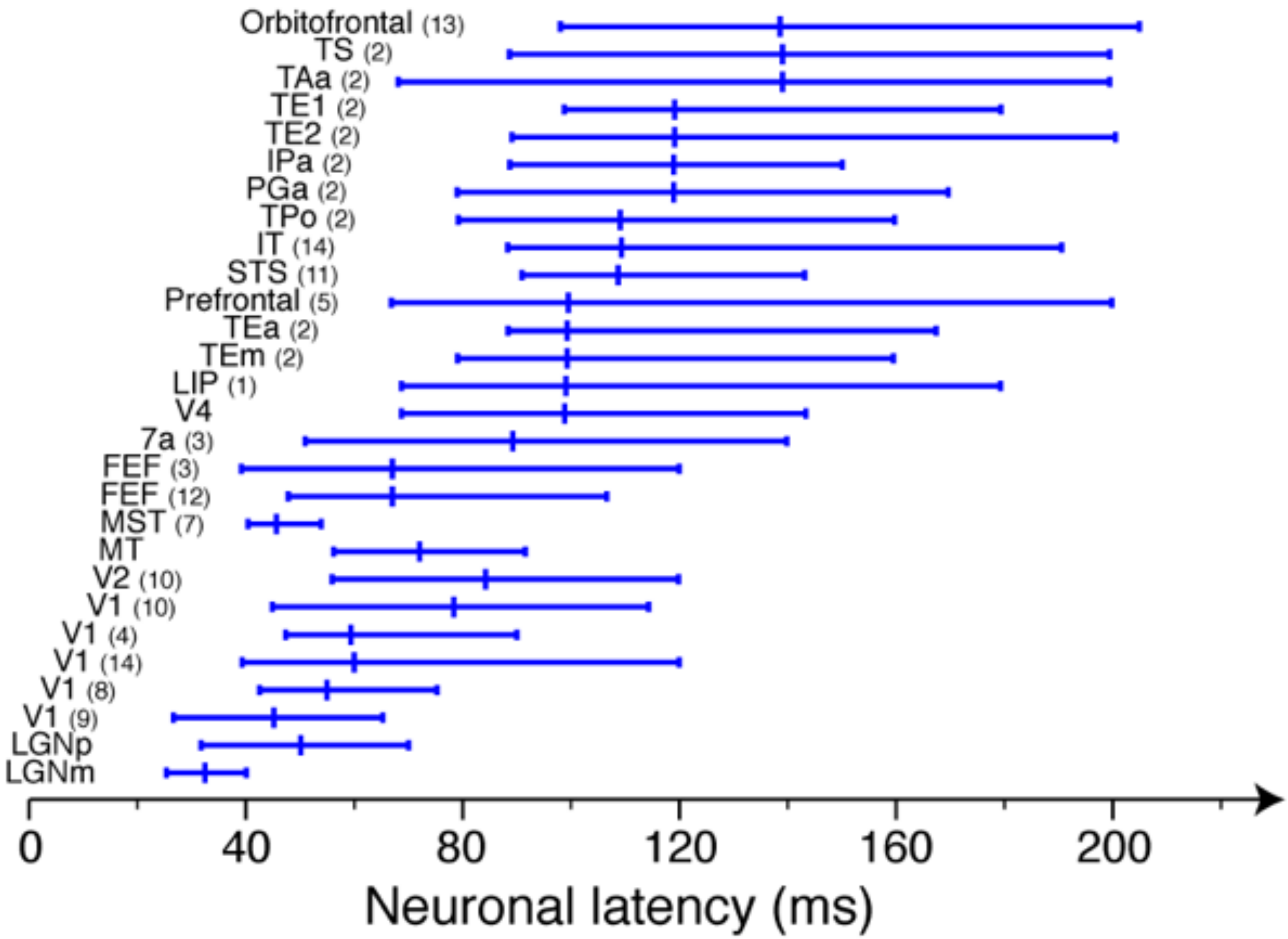

Nowak & Bullier, 1997

Speed of processing in rapid visual categorization

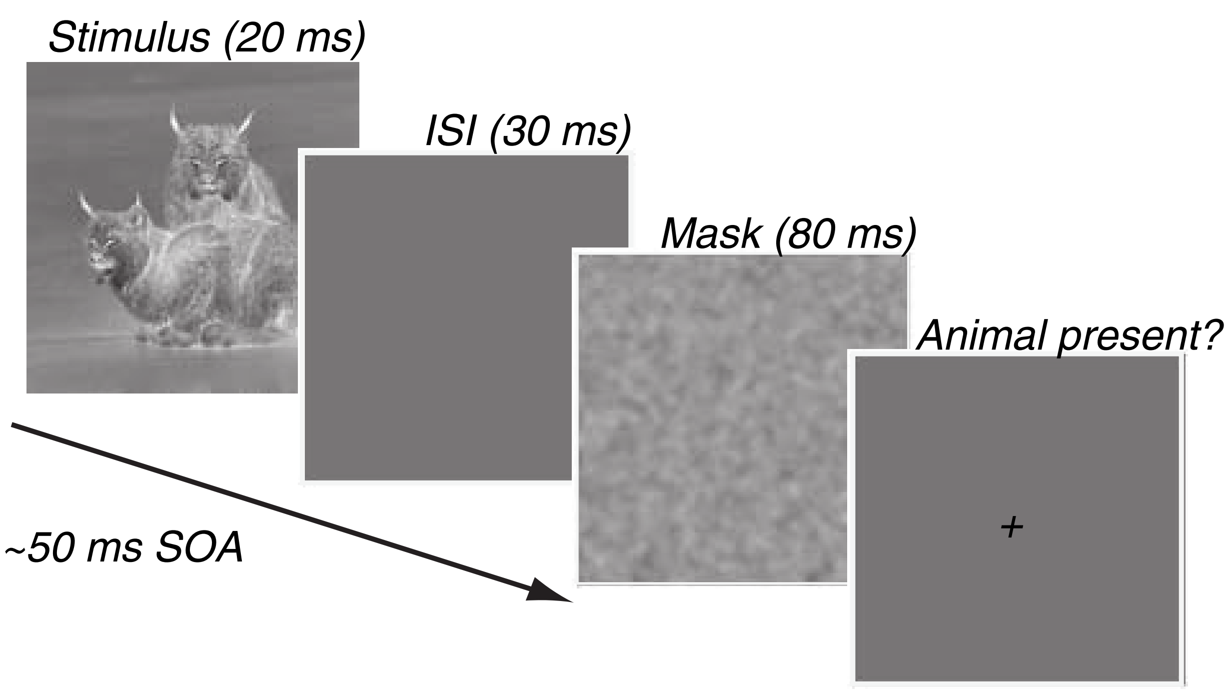

Fabre-Thorpe, Richard & Thorpe, 1998

Speed of processing in rapid visual categorization

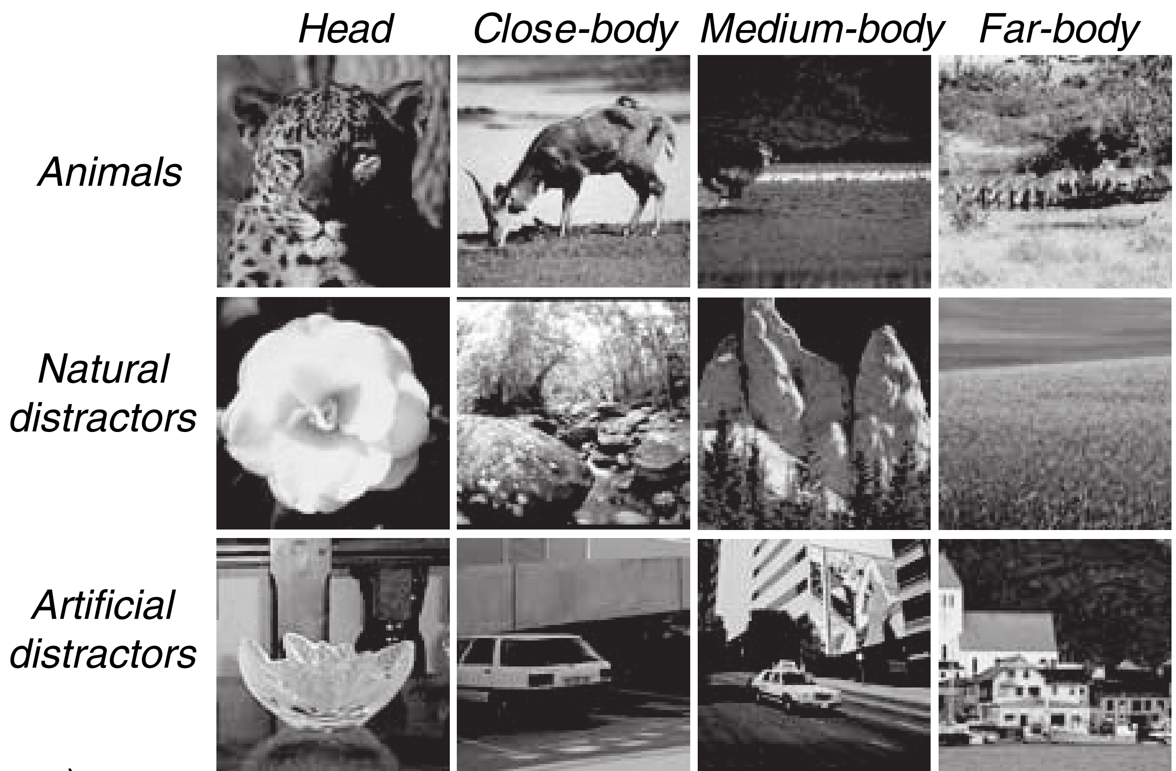

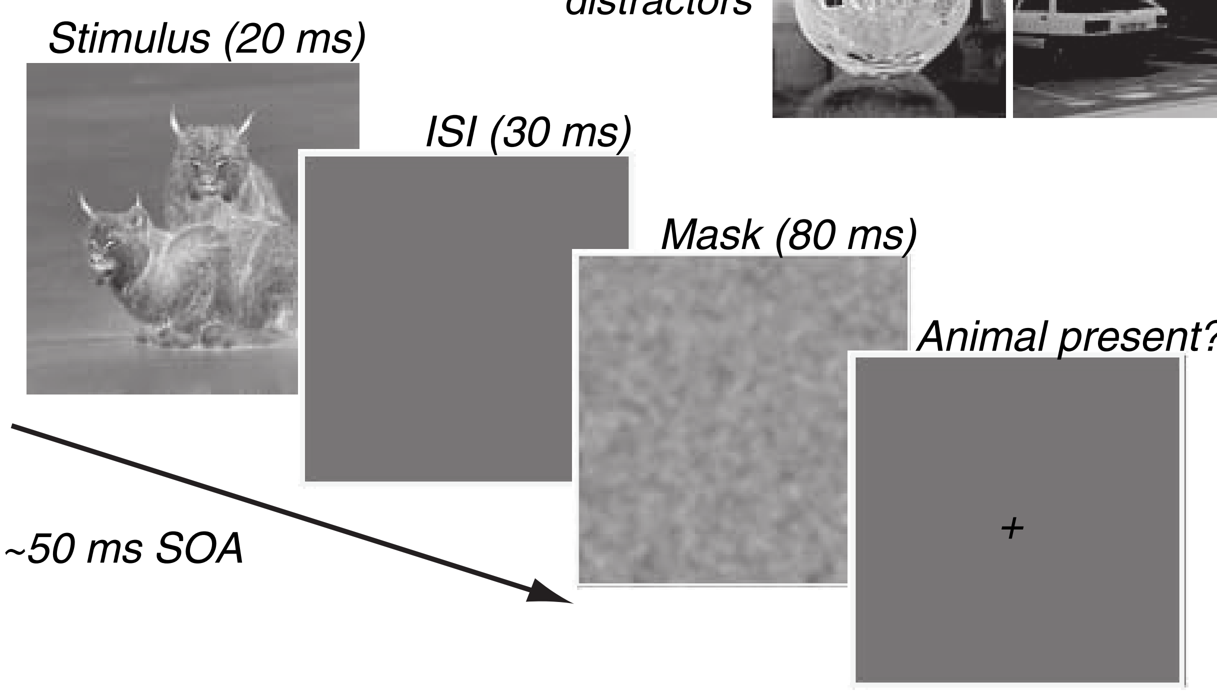

Fabre-Thorpe, Richard & Thorpe, 1998

Speed of processing in rapid visual categorization

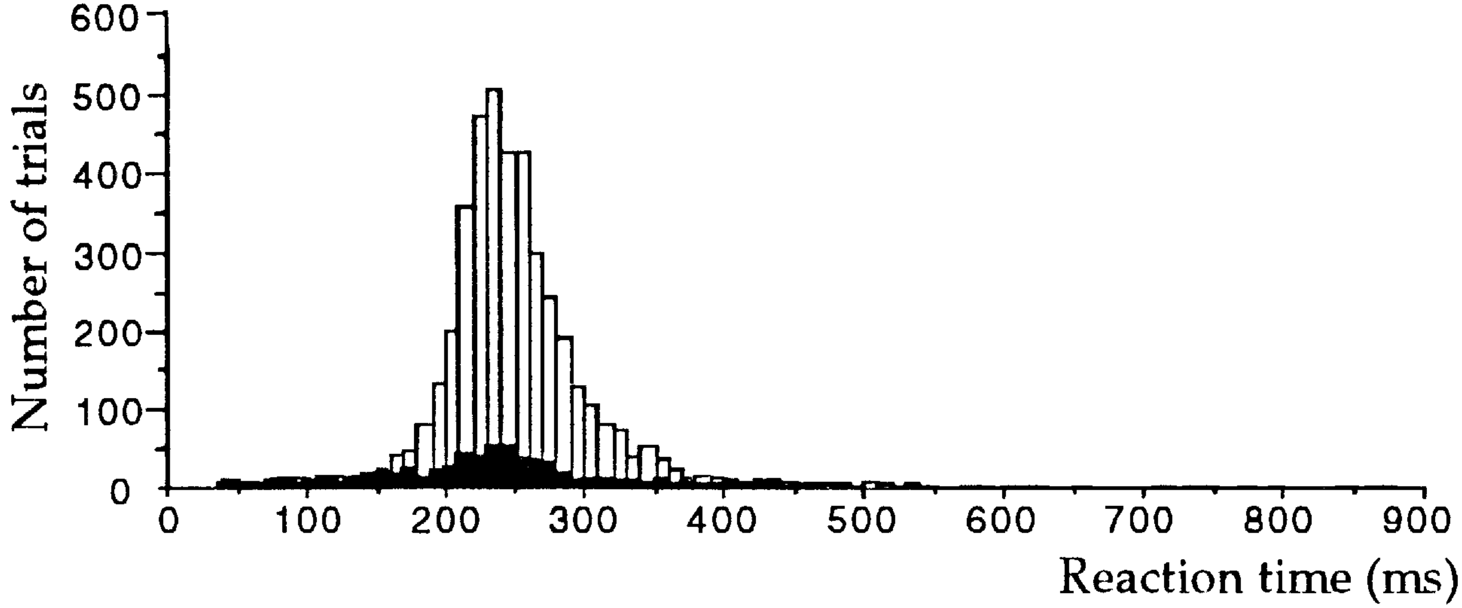

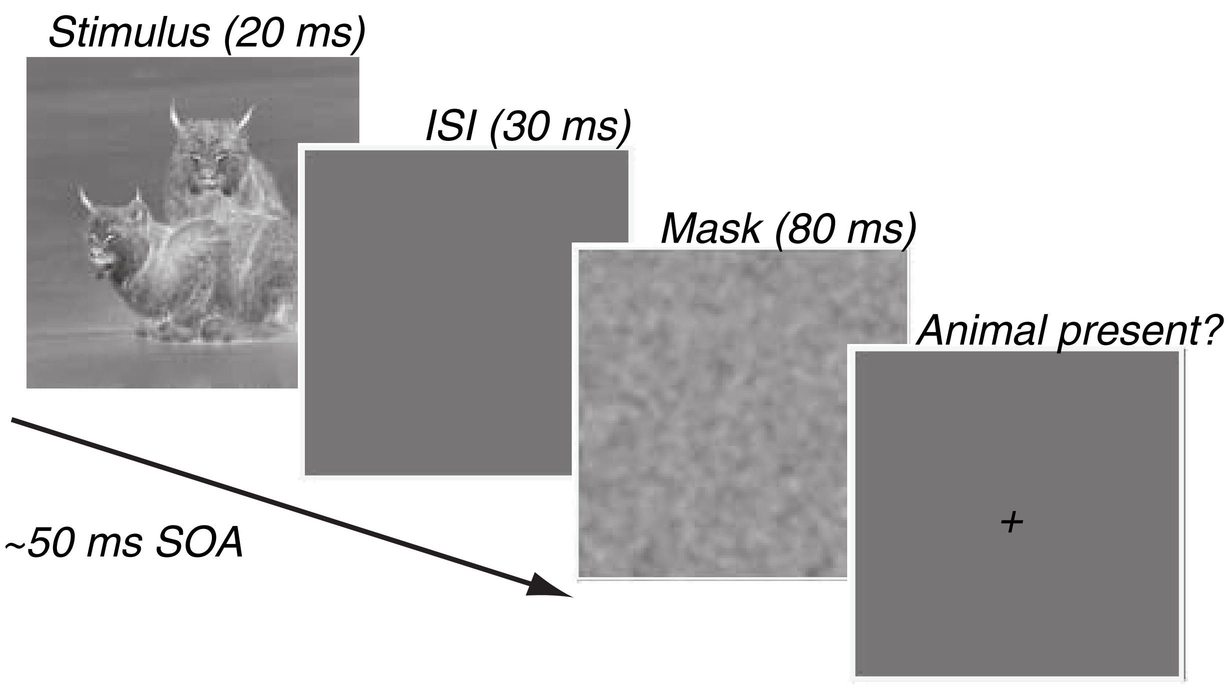

Fabre-Thorpe, Richard & Thorpe, 1998

Cytochrome oxidase labelled stripes in a flattened section of macaque monkey area V2.

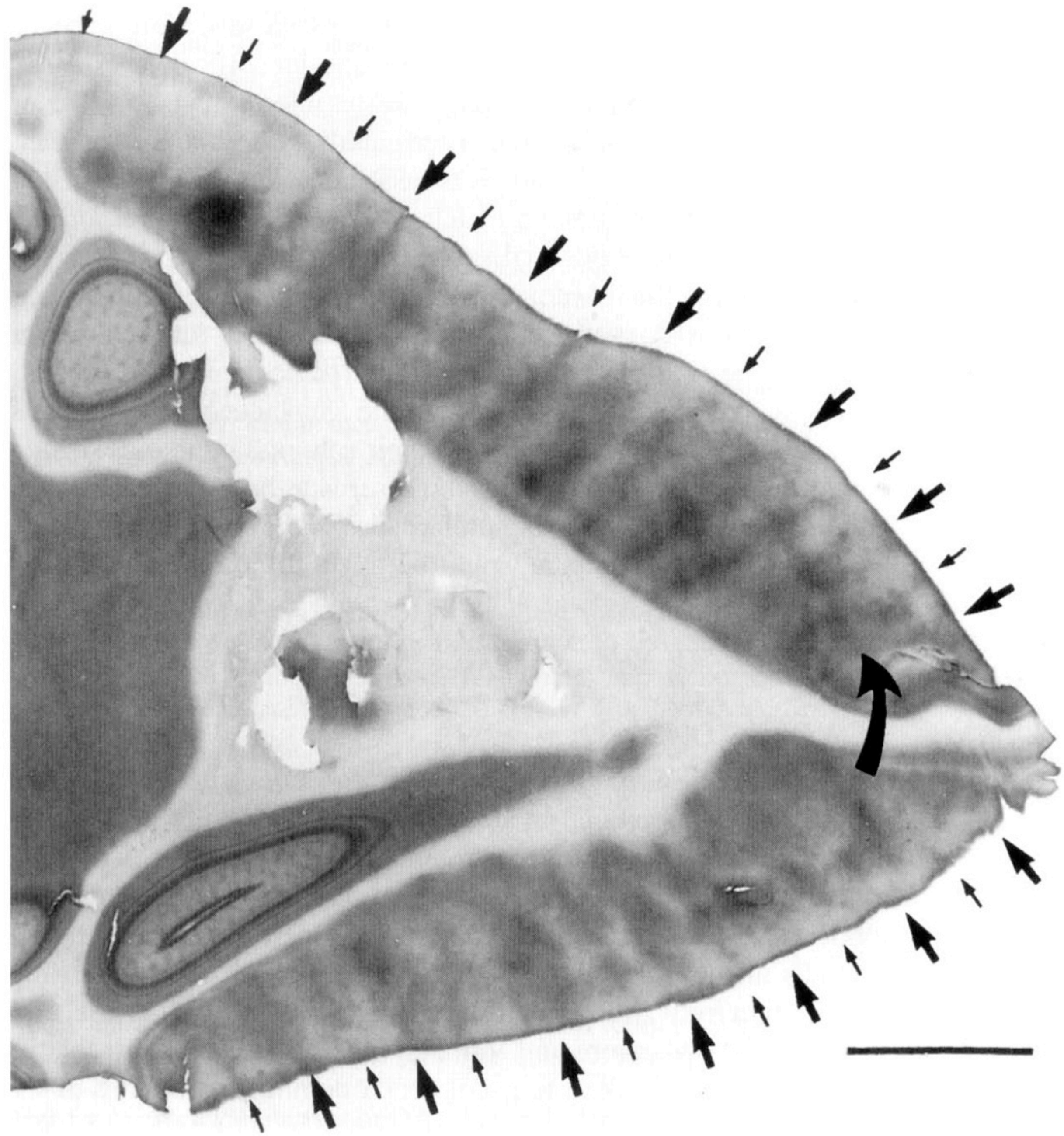

Parallel visual pathways in macaque

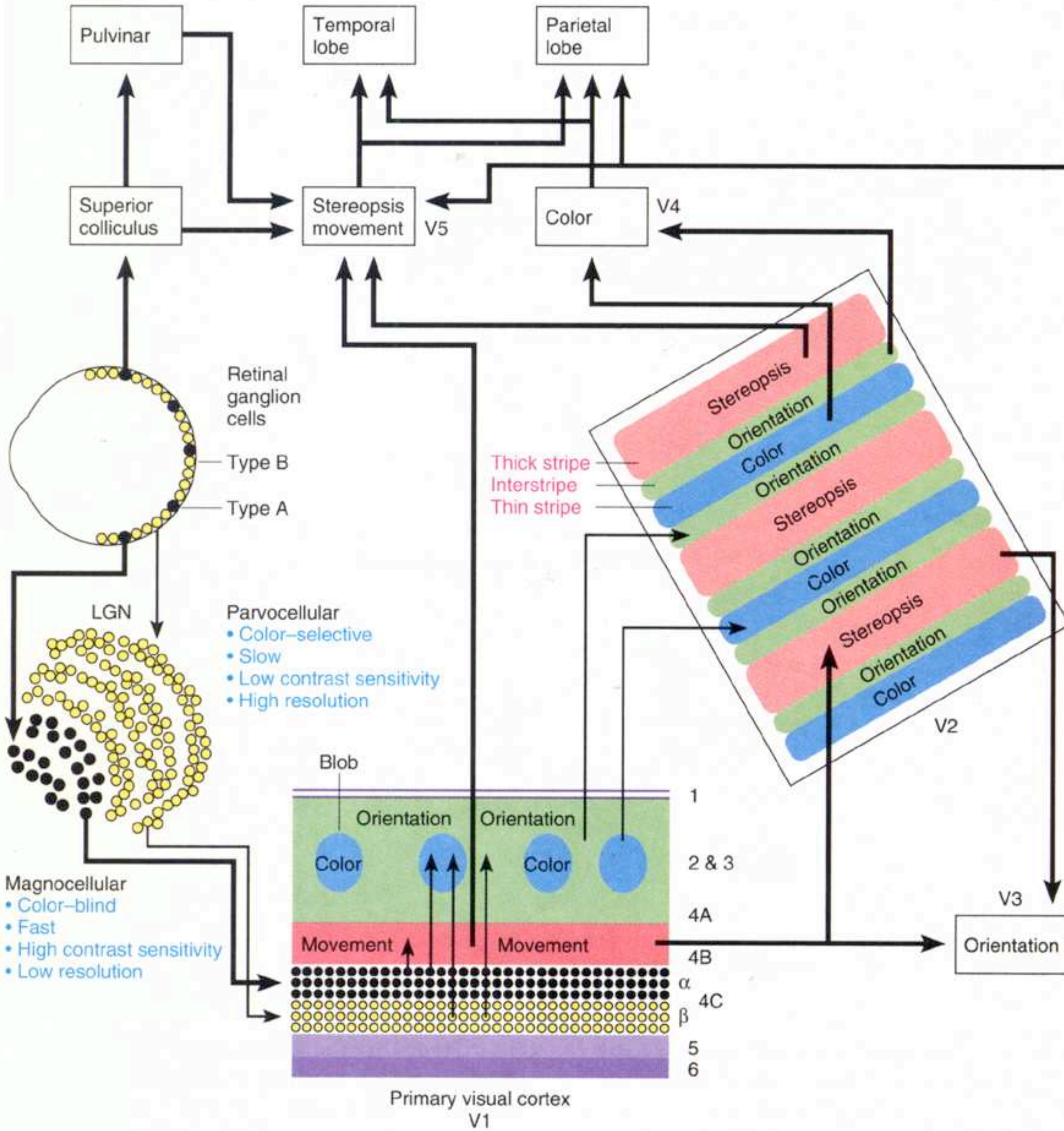

FIGURE 6.36

A summary of the parvocellular and magnocellular visual systems. (Adapted from Livingstone, M., and Hubel, D. *Science*, 1988, *240*, 740–749.)

Geniculate inputs to parallel visual pathways studied with laminar blockade

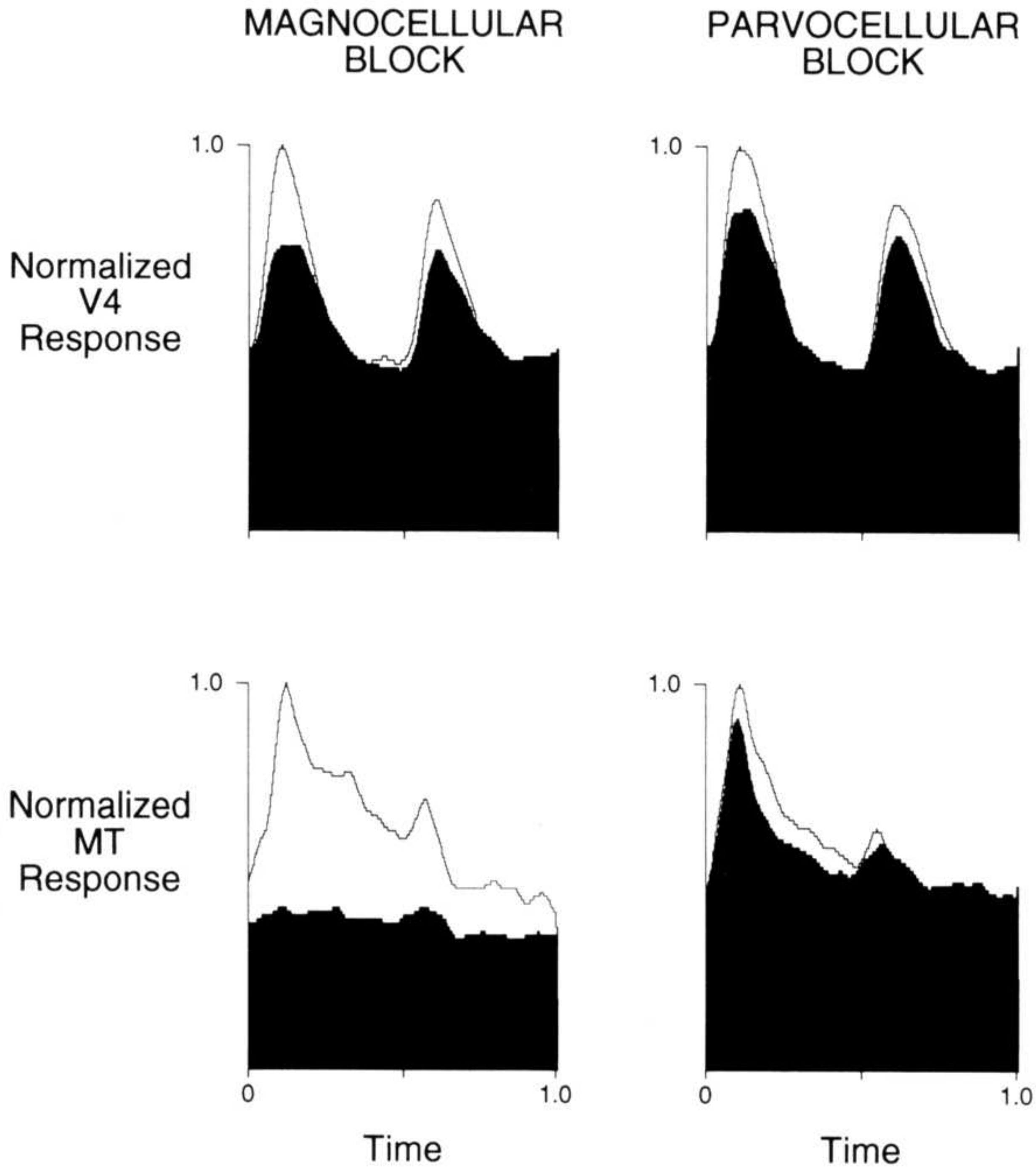

Maunsell, 1990